HHS Public Access

Author manuscript

J Immunol. Author manuscript; available in PMC 2016 April 15.

Published in final edited form as:

J Immunol. 2015 April 15; 194(8): 3784–3797. doi:10.4049/jimmunol.1402960.

Distinct modes of antigen presentation promote the formation, differentiation and activity of Foxp3$^+$ regulatory T cells *in vivo*

Katherine A. Weissler[*], **Victoria Garcia**[*], **Elizabeth Kropf**[*], **Malinda Aitken**[*], **Felipe Bedoya**[*], **Amaya I. Wolf**[*], **Jan Erikson**[*], and **Andrew J. Caton**[*]

Abstract

How the formation and activity of CD4$^+$Foxp3$^+$ regulatory T cells (Tregs) is shaped by TCR recognition of the diverse array of peptide:MHC complexes that can be generated from self- and/or foreign Ags *in vivo* remains poorly understood. We show that a self-peptide with low (but not high) stimulatory potency promotes thymic Treg formation, and can induce conventional CD4$^+$ T cells in the periphery to become Tregs that express different levels of the transcription factor Helios according to anatomical location. When Tregs generated in response to this self-peptide subsequently encountered the same peptide derived instead from influenza virus in the lung-draining lymph nodes of infected mice, they proliferated, acquired a T-bet$^+$CXCR3$^+$ phenotype, and suppressed the antiviral effector T cell response in the lungs. However, these self-Ag-selected Tregs were unable to suppress the anti-viral immune response based on recognition of the peptide as a self-Ag rather than a viral-Ag. Notably, when expressed in a more immunostimulatory form, the self-peptide inhibited the formation of T-bet$^+$CXCR3$^+$ Tregs in response to viral-Ag, and Ag-expressing B cells from these mice induced Treg division without upregulation of CXCR3. These studies show that a weakly immunostimulatory self-peptide can induce thymic and peripheral Foxp3$^+$ Treg formation but is unable to activate self-Ag-selected Tregs to modulate an anti-viral immune response. Moreover, a strongly immunostimulatory self-peptide expressed by B cells induced Tregs to proliferate without acquiring an effector phenotype that allows trafficking from the draining lymph node to the lungs, and thereby prevented the Tregs from suppressing the anti-viral immune response.

Introduction

Regulatory T cells (Tregs) expressing the transcription factor Foxp3 are a subset of CD4$^+$ T cells that are crucial to maintaining immune homeostasis (1, 2). Mice and humans lacking functional Foxp3 develop a rapid autoaggressive lymphoproliferative disease, and there is evidence that the ability of Tregs to maintain immune homeostasis is at least partly a reflection of an intrinsic reactivity of their TCRs toward peptides derived from self-Ags and presented as complexes with the host's MHC Class II molecules (3–6). However, self-Ags can be expressed in differing amounts and by cell types with varying abilities to provide

Correspondence: Andrew J. Caton, 3601 Spruce Street, Philadelphia, PA 19104, Phone: (215) 898-3871, Fax: (215) 898-3868, caton@wistar.org.

[*]The Wistar Institute, Philadelphia, PA 19104, USA

Disclosures

The authors declare no financial conflicts of interest.

costimulation; as a result, they can differ greatly in their immunostimulatory potency for $CD4^+$ T cells (including Tregs), and how this diversity shapes the formation and activity of the Treg repertoire is not yet understood. Moreover, it is clear that $Foxp3^+$ Tregs can participate in and modulate immune responses to pathogens (7), and evidence has emerged that $Foxp3^+$ Tregs can differentiate in response to inflammatory cues (such as cytokines) to acquire novel phenotypes that allow them to selectively modulate qualitatively distinct immune responses (8). At present, how TCR specificity for self- and/or viral-Ag can integrate with inflammatory signals to direct Treg formation and activity *in vivo* remains poorly understood.

Firm evidence that $Foxp3^+$ Tregs can be generated based on specificity for self-Ag came from studies using TCR-transgenic mice showing that recognition of a cognate agonist self-peptide can drive autoreactive thymocytes to undergo deletion and/or to differentiate into $CD4^+CD8^-$ (CD4SP) $Foxp3^+$ thymocytes that are then exported to the periphery (9–11). Although the exact signals that can specify an autoreactive thymocyte to undergo deletion versus development into a $Foxp3^+$ Treg have not yet been defined, there is evidence that relatively high doses of a cognate peptide will induce substantial deletion of autoreactive thymocytes, while lower doses can lead to less thymocyte deletion, and in these circumstances significant formation of $CD4SPFoxp3^+$ cells with specificity for the cognate self-Ag can occur (12, 13). Thymically-derived Tregs (tTregs) appear to constitute the majority of the Treg population (14, 15), but in certain circumstances $CD4^+Foxp3^-$ cells that are present in the periphery can differentiate into $Foxp3^+$ Tregs (termed peripherally-derived Tregs (pTregs)) upon recognition of cognate Ag (16). Evidence for peptide-specific pTreg formation *in vivo* has come primarily from studies involving exogenous administration of cognate Ag, either through injection or feeding, and in some cases, low doses of the peptide were found to favor $Foxp3^+$ pTreg formation (17–20). However, exogenously administered peptides are subject to turnover and clearance, and how specificity for naturally processed self-peptides can direct pTreg formation has not been well studied. Moreover, naturally processed self-peptides can be expressed with varying immunostimulatory potencies, and how this might influence pTreg formation has not been determined.

Tregs have been shown to accumulate at infection sites and suppress the anti-pathogen immune response in multiple different infection models (7). To date, most studies have concluded that Tregs found at sites of infection expanded from pre-existing Tregs, and did not convert from $CD4^+Foxp3^-$ cells following recognition of the pathogen (21–23). However, as outlined above, the pre-immune Treg repertoire appears to be formed based on specificity for self-Ags, and it is unclear how Tregs expressing TCRs that have been selected based on self-reactivity might be able to participate in anti-pathogen immune responses. One possibility is that the Tregs that participate in the immune response to a pathogen underwent initial selection based on the specificity of their TCRs for self-peptide(s), but these TCRs can also cross-react with pathogen-derived Ags. Indeed, several groups have identified naturally-occurring pathogen-specific Tregs at infection sites (21, 24), and others have shown that TCR transgenic Tregs that recognize pathogen-derived Ag were able to modulate the immune responses to both *Mycobacterium tuberculosis* and influenza virus (22, 23). However, an additional possibility is that Tregs can be activated based on TCR recognition

of a selecting self-Ag that is being presented at the site of a viral infection in the context of an inflammatory environment. Once activated, these “self-peptide”-specific Tregs could potentially modulate the development of the anti-viral immune response by bystander effects, although the extent to which such a process can occur during infections is not currently known.

There is also emerging evidence that Tregs can differentiate to acquire unique effector phenotypes following activation (8); these effector phenotypes appear to allow Tregs to respond appropriately to different kinds of inflammatory environment, and their existence has been revealed in part based on studies in mice in which transcription factors that are typically associated with conventional effector $CD4^+$ T cell differentiation have been ablated selectively in $Foxp3^+$ cells (25–27). For instance, ablation of the transcription factor IRF4, which is critical for $CD4^+$ Th2 effector T cell differentiation, led to the spontaneous development of a Th2-mediated immunopathology (25). Likewise, when Tregs specifically lacked Stat3 (which is critical for Th17 cell differentiation), the frequency of IL-17-producing $CD4^+Foxp3^-$ cells was selectively increased and IL-17 dependent inflammatory bowel disease developed (26). Similarly, a functionally specialized subset of Tregs has been identified that express CXCR3 and T-bet (which are otherwise typically associated with conventional $CD4^+$ Th1 cells), and differentiation of these cells was shown to be dependent on IFN-γ and IL-27 signaling through the STAT1 signaling pathway (27). Furthermore, Tregs that lacked T-bet expression were incapable of controlling Th1 cell-mediated immunopathology (27). We previously showed that tTregs that were generated in response to a peptide from the influenza virus hemagglutinin (HA) expressed as a surrogate self-Ag in transgenic mice were able to recognize the same peptide when it was presented as a viral-Ag in influenza virus-infected BALB/c mice, and that the activated tTregs acquired a $T\text{-}bet^+CXCR3^+$ phenotype and suppressed effector T cell activity by acting primarily in the lungs (23). This differentiation of $Foxp3^+$ Tregs into distinct effector types is likely to play a crucial role in coordinating the migration to and/or persistence of Tregs at sites of inflammation (8), but how signals from the TCR and from environmental cues such as cytokines are integrated to mediate Treg differentiation is not well understood.

We have investigated how varying the presentation of an Ag can affect Treg formation and activity *in vivo* using transgenic mice that allow us to follow the fate of T cells with a defined TCR in different contexts. We show that $CD4^+$ T cells that recognize self-Ag outside of the thymus can upregulate Foxp3 and Helios and become functional Tregs, and that self-Ag presented in a less immunostimulatory manner is more conducive to pTreg formation than the same self-Ag presented in a more immunostimulatory manner. Despite promoting Treg formation, this weakly immunostimulatory self-peptide:MHC complex was unable to induce Treg activity during influenza virus infection. Conversely, when the same peptide:MHC complex was derived from an influenza viral-Ag, it drove Tregs to proliferate and acquire a $Tbet^+CXCR3^+$ phenotype, and to suppress the accumulation of $CD4^+Foxp3^-$ and $CD8^+$ effector T cells in the lungs of infected mice. Notably, when this Ag was presented as a highly immunostimulatory self-peptide:MHC complex by targeting its expression to MHC Class II+ APCs, Tregs also underwent substantial proliferation, but little or no differentiation into a $Tbet^+CXCR3^+$ phenotype occurred, and their ability to modulate

an anti-viral immune response was impaired. This failure to promote the formation of $Tbet^+CXCR3^+Foxp3^+$ Tregs could be attributed in part to the presentation of the self-Ag by B cells, and in part to their initial activation in a non-inflammatory environment. Collectively, these studies show that the mode of presentation of a peptide:MHC complex can critically affect the formation, differentiation and activity of $Foxp3^+$ Tregs *in vivo*, and that both the immunostimulatory potency of the Ag and the inflammatory environment that is encountered during initial activation can determine their ability to differentiate into novel effector phenotypes.

Materials and Methods

Mice

TS1, HA28, and HACII mice were previously described and have been backcrossed onto a BALB/c background (9, 28–30). BALB/c.$Foxp3^{eGFP}$ (31) mice and congenic BALB/c.Ly5.1 mice were from The Jackson Laboratory. Mice were inter-mated to produce TS1.$Foxp3^{eGFP}$.Ly5.1 mice and TS1xHA28.$Foxp3^{eGFP}$.Ly5.1 mice. When transgenes were expressed, experimental mice were heterozygous for the TCR transgene, HA transgene, and Ly5.1 allele, and were homozygous for the $Foxp3^{eGFP}$ reporter. BALB/c mice were from Charles River Laboratories. Mice were housed under specific pathogen-free conditions in the Wistar Institute Animal Facility, and experiments were performed according to protocols approved by the Wistar Institutional Animal Care and Use Committee.

Influenza viruses and infections

The influenza viruses PR8 (A/Puerto Rico/8/1934 [H1N1]) and its derivative RV6, which contains a single amino acid substitution in the Site 1 peptide of PR8 HA (32, 55), were propagated in 10-d hen's embryonated eggs. For infection, mice were anesthetized by i.p. injection of ketamine/xylazine (70/7 mg/kg), and 0.003 HAU of PR8 virus or 0.005 HAU of RV6 virus was administered intranasally in 50 μL PBS.

FACS and adoptive cell transfer

For Treg induction experiments, $6.5^+CD4^+CD25^-eGFP^-$ cells were purified from the LNs and spleens of TS1.$Foxp3^{eGFP}$.Ly5.1 mice by cell sorting. For Treg transfer experiments, $CD4^+eGFP^+$ cells were isolated from the LNs and spleens of TS1xHA28.$Foxp3^{eGFP}$.Ly5.1 mice. In both cases, 10^6 cells were adoptively transferred into recipients via tail vein injection. FACS was performed using a MoFlow (DakoCytomation) or FACSAria (BD Biosciences). In some instances, cells were labeled with CellTrace Violet (Invitrogen) at 3μM for 20 minutes then washed prior to transfer.

Cell isolation

Mice were euthanized using CO_2, and 4 mL PBS was injected into the right ventricle of the heart to perfuse the lungs. Lungs were then removed, cut into small pieces, and incubated at 37 °C in IMDM plus 10% FBS supplemented with collagenase D (350 U/lung) and DNase I (350 μg/lung; both from Roche Diagnostic) for 1 hour.

Cell staining and flow cytometry

Single cell suspensions of pLNs (pooled axillary, brachial, and inguinal), mesenteric LNs, spleens, thymi, mediastinal LNs and lungs were stained using the Live/Dead Fixable Aqua Dead Cell Stain Kit (Invitrogen), blocked with Fc block (BD Biosciences), then stained for surface markers at 4 °C for 25 minutes. Allophycocyanin-conjugated H-2K^{d}:Np147 tetramer was directly added to the primary Ab dilution, and cells were incubated for 1 hour at 4 °C. For intracellular staining, cells were fixed and permeabilized after surface staining using the Foxp3/Transcription Factor Staining Buffer Set (eBioscience) according to manufacturer's instructions. Antibodies were purchased from eBioscience, BD Biosciences, or Invitrogen. Data was collected using an LSR II flow cytometer (BD Biosciences) and analyzed on FlowJo software (Tree Star).

In vitro Treg suppression assay

In a 96-well U-bottom plate, 100,000 CD4^{-}CD8^{-} BALB/c splenocytes, 50,000 FACS-isolated 6.5^{+}CD4^{+}eGFP^{-} responder cells from TS1.Foxp3 mice, and 1 μM S1 peptide were combined in supplemented IMDM plus 10% FBS. 6.5^{+}CD8^{-}eGFP^{+}Ly5.1^{+} Tregs were isolated from TS1xHA28. Foxp3^{eGFP}.Ly5.1 mice or from HA28 recipient mice at d 7 post-transfer of 6.5^{+}CD4^{+}CD25^{-}eGFP^{-} cells from TS1.Foxp3^{eGFP}.Ly5.1 mice; these Tregs were added to the culture at a 1:2 or 1:4 ratio relative to the responder cells. Cells were stained for flow cytometric analysis after 3 d of culture.

In vitro APC:T cell coculture

B cells (CD19^{+}CD11c^{-}CD11b^{-}), dendritic cells (DCs) (CD19^{-}CD11c^{+}Ly6C^{-}Ly6G^{-}), neutrophils (CD19^{-}CD11c^{-}CD11b^{+}Ly6G^{hi}Ly6C^{lo}) and inflammatory monocytes (CD19^{-}CD11c^{-}CD11b^{+}Ly6G^{-}Ly6C^{hi}) were isolated from the mediastinal LNs of mice at d 6 post-infection (p.i.). These APCs were plated in a 96 well U-bottom plate either undiluted, or diluted into CD4^{-}CD8^{-} feeder cells from the spleen of a BALB/c mouse, such that 100,000 cells were present in each well in supplemented IMDM plus 10% FBS. 60,000 cells isolated from the LNs of a TS1xHA28.Foxp3^{eGFP} mouse and labeled with CellTrace Violet were then added to each well and cultured for 4 d of culture at 37 °C.

Real-time quantitative RT-PCR

RNA was isolated from harvested tissue using a Biospec Tissue Tearor and TRIzol reagent (Life Technologies), and purified and concentrated using an RNeasy kit (Qiagen). cDNA was synthesized with the High Capacity RNA to cDNA kit (Applied Biosystems), and RT-qPCR was performed using TaqMan Gene Expression Master Mix (Applied Biosystems) on a 7500 Fast Real-Time PCR system.

ELISA for IFN-γ

Blood was collected immediately post-mortem by cardiac puncture, allowed to clot, then spun down to separate out serum. To perform the ELISA, a 96-well plate was coated with anti-IFN-γ antibody (clone R4-6A2; BD Biosciences) overnight. Serum was plated undiluted and diluted 1:3 with PBS supplemented with 10% FBS. Biotinylated-anti-IFN-γ (clone XMG1.2; eBioscience) was used as the secondary antibody, and streptavidin-HRP

and tetramethylbenzidine (eBioscience) were used to detect bound antibody, and the concentration was calculated based on a standard curve using an IFN-γ standard.

Statistical methods

Statistical tests were performed with GraphPad Prism software. A one-way ANOVA followed by Tukey's post-test was used for comparisons between groups within the same dataset. A two-tailed Student *t* test was used where indicated when comparing two independent groups.

Results

Stimulatory potency of the HA self-Ag determines the extent of autoreactive thymocyte deletion and Treg formation

HA28 and HACII mice are previously described transgenic mouse lineages in which sequences derived from the influenza virus PR8 HA are expressed under the control of different promoter/enhancer sequences. In HA28 mice, the SV40 early region promoter/enhancer drives expression of a truncated polypeptide corresponding to the NH_2-terminal 273 amino acids of the PR8 HA polypeptide, and studies using bone marrow chimeras have shown that this polypeptide is expressed in radioresistant cell types (9, 12, 29, 33, 34). By contrast, the I-E^a MHCII promoter directs transgene expression in HACII mice, and flow cytometric studies have demonstrated cell surface expression of the HA selectively by MHC Class II+ cells (35). The two lineages also differ in the amount of transgene mRNA that is expressed, with substantially higher levels of HA mRNA being found in lymphoid tissues and intestine of HACII mice relative to HA28 mice (Fig. 1A). To assess how these differences in expression affect the ability of the HA self-Ag to stimulate $CD4^+$ T cells, we injected CellTrace Violet-labeled HA-specific $CD4^+$ T cells from TS1 mice (which are transgenic mice expressing an HA-specific TCR that can be recognized by the anti-clonotypic mAb 6.5 (36)) into BALB/c, HA28 and HACII mice and analyzed the extent of their proliferation in pooled LNs 5 d after transfer (Fig. 1B). All of the 6.5^+CD4^+ T cells remained undivided in BALB/c mice, while in HA28 mice, some of the cells remained undivided, while others had undergone up to 5 divisions. By contrast, in HACII mice, all of the transferred cells had proliferated, and most of the cells had undergone more rounds of division than had occurred in HA28 mice. Thus, the HA is a more potently immunostimulatory self-Ag in HACII mice than in HA28 mice, most likely because of the higher levels of HA mRNA and targeted expression of the HA transgene to MHC Class II^+ cells.

To evaluate how these differences in immunostimulatory potency can influence autoreactive thymocyte development, we mated HA28 and HACII mice with TS1 mice to produce TS1xHA28 and TS1xHACII mice, and analyzed 6.5^+CD4SP thymocyte development. There was a significant decrease in the number of 6.5^+CD4SP thymocytes in TS1xHA28 mice relative to TS1 mice, but the number of $6.5^+CD4SPFoxp3^+$ thymocytes was significantly increased, consistent with previous studies showing that the presence of the self-HA can induce both 6.5^+CD4SP thymocyte deletion and $6.5^+CD4SPFoxp3^+$ thymocyte formation in TS1xHA28 mice (9, 12) (Fig. 1C). By contrast, far fewer 6.5^+CD4SP thymocytes were

present in TS1xHACII mice relative to either TS1 or TS1xHA28 mice. Although the percentage of 6.5^+CD4SP thymocytes that were $Foxp3^+$ was increased, the severe deletion of 6.5^+CD4SP thymocytes meant that the number of 6.5^+CD4SP$Foxp3^+$ thymocytes was no higher in TS1xHACII mice than in TS1 mice (Fig. 1C). The relative representations of 6.5^+CD4^+ and $6.5^+CD4^+Foxp3^+$ cells in non-gut associated (brachial, axillary and inguinal) peripheral LNs (pLNs) of TS1, TS1xHA28 and TS1xHACII mice broadly paralleled those of 6.5^+CD4SP thymocytes, with the exception that 6.5^+CD4^+ T cells were no less abundant in TS1xHA28 mice than in TS1 mice, suggesting that homeostatic processes occurring in the periphery can compensate for the reduced frequencies caused by thymocyte deletion (Fig. 1D). Collectively, these studies show that differences in the immunostimulatory potency with which the self-HA is expressed can cause significant differences both in its ability to induce activation of conventional $CD4^+$ T cells, and in the extent to which it induces deletion of HA-specific thymocytes. Moreover, because of these effects, the HA self-Ag is better at promoting the formation of $6.5^+CD4^+Foxp3^+$ Tregs in TS1xHA28 mice, since it does not induce the extensive deletion that occurs in response to the more stimulatory form of HA that is expressed in TS1xHACII mice.

The extent of $CD4^+Foxp3^-$ T cell conversion to $Foxp3^+$ Tregs depends on the stimulatory potency of the self-Ag

Previous studies have variously shown that mature $CD4^+$ T cells are capable of undergoing expansion, deletion and/or conversion into $Foxp3^+$ Tregs upon antigenic stimulation in the periphery (37, 38). To assess how differences in the expression of self-HA in HA28 and HACII mice might influence these different fates, we purified congenically-marked $6.5^+CD4^+Ly5.1^+CD25^-eGFP^-$ cells from the LNs of TS1.$Foxp3^{eGFP}$.Ly5.1 mice (the $Foxp3^{eGFP}$ reporter allele was used to purify $Foxp3^-$ cells based on the absence of eGFP expression), labeled the cells with CellTrace Violet, and transferred them into BALB/c, HA28, or HACII hosts (Fig. 2A). Three days after transfer we examined the extent of division and eGFP upregulation (as an indication of Foxp3 expression) of 6.5^+CD4^+ cells in pLNs. While the 6.5^+CD4^+ T cells in the pLNs of BALB/c mice remained undivided and had not upregulated Foxp3 expression, many of the 6.5^+CD4^+ cells isolated from the pLNs of HA28 mice had undergone several rounds of division, and a significantly higher percentage of these cells expressed Foxp3 compared to those isolated from BALB/c mice (Fig. 2B). Moreover, most of the 6.5^+CD4^+ cells that had upregulated Foxp3 in HA28 mice either remained undivided or had undergone one or two divisions, while those that had proliferated to a greater extent were mostly $Foxp3^-$. By contrast, all 6.5^+CD4^+ T cells in HACII recipient mice had undergone multiple rounds of division, but the percentage that had upregulated Foxp3 expression was no higher than in BALB/c mice (Fig. 2B).

Using the same adoptive transfer protocol, we assessed the accumulation and Foxp3 expression of $CD4^+Ly5.1^+$ cells at later time points. In HA28 mice, similar numbers of $CD4^+Ly5.1^+Foxp3^+$ T cells were recovered at d 7 after transfer as had been obtained 3 d after transfer (Fig. 2B). By contrast, approximately 3 times as many $CD4^+Ly5.1^+$ T cells were recovered in HACII mice at 7 d post-transfer compared to 3 d post-transfer, but there was again negligible accumulation of $CD4^+Ly5.1^+Foxp3^+$ T cells. When we initially analyzed HA28 and HACII mice at 14 and 21 d post-transfer, we found that recoveries were

variable and that some mice contained no $CD4^+Ly5.1^+$ cells, while there were good recoveries from other individual mice. One explanation for this irreproducibility could be that the $Ly5.1^+$ cells were being rejected because expression of GFP by $CD4^+$ T cells was in some individuals promoting formation of GFP-specific $CD8^+$ T cells that were rejecting the transferred cells. Accordingly, we repeated the d 14 and d 21 transfers of $CD4^+Ly5.1^+Foxp3^-$ cells into BALB/c.$Foxp3^{eGFP}$, HA28.$Foxp3^{eGFP}$, and HACII.$Foxp3^{eGFP}$ mice, and in this setting we obtained consistent and equivalent recoveries of $CD4^+Ly5.1^+$ cells from all of the individual mice within a group. Indeed, similar numbers of $CD4^+Ly5.1^+$ cells were recovered 21 d after transfer into HA28.$Foxp3^{eGFP}$ and BALB/c.$Foxp3^{eGFP}$ mice, but nearly half of the cells recovered from HA28.$Foxp3^{eGFP}$ mice expressed Foxp3, while no Foxp3 expression was detected in $CD4^+Ly5.1^+$ T cells recovered from BALB/c mice (Fig. 2B). By contrast, in HACII.$Foxp3^{eGFP}$ mice, sizable populations of $CD4^+Ly5.1^+$ T cells were recovered 21 d after transfer, and there again was little or no expression of Foxp3 by these cells. Since previous studies have identified APCs in gut mucosal tissue that promote $Foxp3^+$ Treg formation (18, 19), we also assessed $Ly5.1^+$ cell accumulation and Foxp3 upregulation in the mesenteric LN (mesLN) in all of these experiments. The extent of $CD4^+Ly5.1^+$ T cell accumulation and of Foxp3 upregulation was similar in the mesLN relative to non-gut-draining pLNs (Supplemental Fig. 1). Thus, expression of the HA as a self-Ag with a low stimulatory potency is optimal for inducing the formation of $CD4^+Foxp3^+$ T cells from conventional $CD4^+Foxp3^-$ T cells in the periphery.

To further characterize the $CD4^+Foxp3^+$ T cells that were being formed in response to the HA self-Ag in HA28 mice, we examined expression of the transcription factor Helios, which is expressed by $Foxp3^+$ Tregs that have been formed intrathymically, but has been found in some studies to not be expressed by $Foxp3^+$ Tregs that have been formed in the periphery (39, 40). Helios was progressively upregulated in $CD4^+Ly5.1^+Foxp3^+$ T cells isolated from HA28 mice such that by d 14 post-transfer, the majority of the $CD4^+Ly5.1^+Foxp3^+$ T cells were $Helios^+$ (Fig. 2C). Notably, the $CD4^+Ly5.1^+$ T cells that had not acquired Foxp3 expression appeared to transiently upregulate Helios relative to cells that had been transferred into BALB/c mice at early times post-transfer, but by d 14 and 21 these cells no longer expressed significant levels of Helios. Since the formation of $CD4^+Foxp3^+Helios^-$ pTregs has mostly been described in systems in which Ags had been administered orally (39, 41), we also examined Helios levels on $CD4^+Ly5.1^+Foxp3^+$ T cells that had been isolated from the mesLNs of HA28 mice. Interestingly, the mesLN contained significantly higher percentages of $CD4^+Ly5.1^+Foxp3^+$ T cells that were $Helios^-$ than the non-gut-draining pLN (Fig. 2D). Since more than 90% of the $CD4^+Ly5.1^+Foxp3^+$ cells isolated from each site expressed the 6.5 clonotypic TCR, this indicates that factors other than TCR specificity must determine the extent of Helios upregulation by $CD4^+Foxp3^+$ T cells that have been generated in gut- versus non-gut-associated LNs.

Finally, to determine the suppressive capacity of the $CD4^+Foxp3^+$ T cells that were formed in HA28 mice, we re-isolated $6.5^+Ly5.1^+eGFP^+$ cells from the pLNs of HA28 mice at d 7 post-transfer. These purified cells were then incubated for 3 d *in vitro* with S1 peptide and APCs, and compared with tTregs (i.e. $6.5^+Ly5.1^+eGFP^+$ Tregs from TS1xHA28.$Foxp3^{eGFP}$ mice) for their expression of Foxp3 and for their ability to suppress proliferation of co-

cultured $6.5^+CD4^+Ly5.1^-Foxp3^{eGFP-}$ responder T cells from TS1.$Foxp3^{eGFP}$ mice. In the cultures containing cells that had acquired Foxp3 expression following transfer into HA28 mice (pTregs), there was a higher percentage of $CD4^+Ly5.1^+$ cells that appeared to have lost Foxp3 expression than was the case for the cultures containing tTregs from TS1xHA28.eGFP mice (Fig. 2E). Nevertheless, more than 75% of the $CD4^+Ly5.1^+$ pTregs maintained eGFP expression, and were as effective as tTregs in suppressing the proliferation of $CD4^+Ly5.1^-$ responder T cells.

Self-HA does not promote Treg activity during an influenza virus infection

The HA can also be expressed as a viral-Ag that is recognized by 6.5^+CD4^+ T cells during an infection with the PR8 strain of influenza virus; as we previously reported, HA expressed as a viral-Ag in PR8-infected BALB/c mice induced $6.5^+CD4^+Foxp3^-$ cells from TS1.$Foxp3^{eGFP}$ mice to proliferate, but not to differentiate into $Foxp3^+$ pTregs, which contrasts with the ability of self-HA to induce 6.5^+ pTreg formation in HA28 mice (Supplementary Fig. 2) (23). Although it was unable to induce the formation of 6.5^+ pTregs, we showed that the HA viral-Ag could activate 6.5^+ tTregs that had been generated in TS1xHA28 mice to modulate the anti-viral immune response (23). In order to examine whether the HA might similarly activate 6.5^+ tTregs to suppress the anti-viral immune response when it is recognized as a self- rather than a viral-Ag, we repeated these studies using a mutant virus (RV6), which bears a single amino acid substitution in the S1 determinant of HA (i.e. the peptide recognized by the 6.5 TCR) that impairs recognition of the viral-Ag by the transferred Tregs (32). $CD4^+Ly5.1^+Foxp3^+$ Tregs from TS1xHA28.$Foxp3^{eGFP}$.Ly5.1 mice were transferred into HA28 or BALB/c mice, which were then infected with RV6 virus, as well as into BALB/c mice that were subsequently infected with PR8 virus (Fig. 3A). Since RV6 and PR8 induce similar degrees of weight loss and serum IFN-γ levels when used to infect BALB/c or HA28 mice (Fig. 3B,C), the extent to which the self-HA Ag can activate HA-specific Tregs could be assessed by comparison of Treg-recipient RV6-infected HA28 mice (in which the Tregs can recognize the self-HA peptide, but react poorly with the viral-Ag) with Treg-recipient RV6-infected BALB/c mice (which do not express the HA self-Ag), and with Treg-recipient PR8-infected BALB/c mice (in which the transferred Tregs can recognize the HA as a viral-Ag, but not as a self-Ag).

Conventional $CD4^+$ T cell responses to infectious agents are typically initiated in the LNs that drain the infected tissue (42). Similarly, we found that $6.5^+CD4^+Foxp3^+$ Tregs had undergone multiple rounds of division in the lung-draining mediastinal lymph nodes (medLNs) of PR8-infected BALB/c mice at d 5 post-infection (p.i.), followed at d 8 p.i. by a dramatic increase in the number of $6.5^+CD4^+Foxp3^+$ Tregs in the lungs (Fig. 3D). By contrast, far fewer $6.5^+CD4^+Foxp3^+$ Tregs were present in either the medLNs or the lungs when these cells had been transferred into RV6-infected BALB/c mice, reflecting the reduced reactivity of the 6.5 TCR toward the RV6 mutant (Fig. 3D). Notably, even though HA28 mice expressed the HA as a self-peptide in the medLNs (as evidenced by the division of 6.5^+ Tregs in uninfected HA28 mice), 6.5^+ Treg numbers were similar in RV6-infected HA28 and BALB/c mice (Fig. 3D). Thus, even though interactions with the HA self-Ag can promote the formation and persistence of $6.5^+CD4^+Foxp3^+$ Tregs in HA28 mice, they did

not direct 6.5$^+$ Tregs to accumulate in the lungs during an infection with a non-cognate influenza virus.

We also previously showed that 6.5$^+$CD4$^+$Foxp3$^+$ Tregs can differentiate into T-bet$^+$Foxp3$^+$ Tregs in PR8-infected BALB/c mice (23). Consistent with these studies, the 6.5$^+$CD4$^+$Foxp3$^+$ Tregs that had undergone division in the medLNs of PR8-infected BALB/c mice at d 5 p.i. had upregulated CXCR3 and contained cells with increased T-bet expression, and upregulation of CXCR3 and T-bet was also observed in the lungs of PR8-infected BALB/c mice at d 8 p.i. (Fig. 4A–C). By contrast, significantly lower percentages of the 6.5$^+$CD4$^+$Foxp3$^+$ Tregs had upregulated CXCR3 or T-bet in RV6-infected BALB/c or HA28 mice (Fig. 4A–C). To examine whether the presence of differentiated Tregs was modifying the antiviral immune response, we determined the frequencies of CD4$^+$Foxp3$^-$ and CD8$^+$ effector cells, and of CD8$^+$ T cells that could recognize the H-2K^d:NP147 epitope of the viral nucleoprotein (as determined by tetramer staining), in the lungs of mice that had or had not received 6.5$^+$CD4$^+$Foxp3$^+$ Tregs from TS1xHA28 mice. In the absence of transferred Tregs, the magnitudes of the CD4$^+$Foxp3$^-$ and CD8$^+$ effector T cell responses were similar between all of the mice irrespective of whether they had been infected with PR8 or RV6. Only in PR8-infected BALB/c mice that received 6.5$^+$CD4$^+$Foxp3$^+$ Tregs was a decrease in the effector T cell response observed (Fig. 4D,E). Thus, interactions with the HA self-Ag did not direct 6.5$^+$ Tregs to differentiate or limit effector T cell accumulation in the lungs during an infection with a non-cognate influenza virus, whereas 6.5$^+$ Tregs that could recognize HA as a viral-Ag did differentiate and suppress the accumulation of effector cells.

A strongly immunostimulatory self-Ag inhibits Treg differentiation during influenza virus infection

It was possible that 6.5$^+$ Tregs expanded and suppressed the immune response following recognition of viral-Ag in a PR8 virus-infected BALB/c mouse, but not following recognition of self-Ag during an RV6 virus infection in an HA28 mouse, because Treg proliferation and activation require the high levels of the HA Ag that are generated during infection. To test whether increasing the stimulatory potency of the HA as a self-Ag could promote 6.5$^+$ Treg activity in virus-infected mice, we transferred 6.5$^+$CD4$^+$Foxp3$^+$ Tregs from TS1xHA28.Foxp3^{eGFP}.Ly5.1 mice into HACII mice (in which the HA is a strongly immunostimulatory self-Ag), and infected these mice with the weakly crossreactive RV6 virus. As controls, we introduced the Tregs into BALB/c or HACII mice and infected these mice with PR8 virus, and also analyzed HACII mice that had received Tregs but were not infected (Fig. 5A). At d 5 p.i., the Ly5.1$^+$ Tregs in the medLNs and lungs of both uninfected and RV6-virus infected HACII mice had undergone similar levels of division as the Tregs in PR8-infected BALB/c mice, suggesting that the self-HA in the medLN and lungs of HACII mice was equally capable of inducing division of 6.5$^+$ Tregs as was the virus-derived PR8 HA (Fig. 5B). Notably, however, at d 8 p.i., significantly fewer CD4$^+$Ly5.1$^+$Foxp3$^+$ cells had accumulated in the medLNs of either uninfected or RV6-infected HACII mice than occurred in PR8-infected BALB/c mice, and these cells also expressed significantly lower levels of CXCR3 and T-bet than were found in PR8-infected BALB/c mice (Fig. 5C–E). Consistent with impaired differentiation, fewer CD4$^+$Ly5.1$^+$Foxp3$^+$ cells accumulated in the

lungs of either uninfected or RV6-infected HACII mice, and the cells that did accumulate again expressed lower levels of T-bet compared to those in PR8-infected BALB/c mice (Fig. 5C–E).

Unexpectedly, when we examined the ability of 6.5^+ Tregs to differentiate in HACII mice that had been infected with PR8 virus, we found that the accumulation of $CD4^+Ly5.1^+Foxp3^+$ cells in the medLN and lungs was again significantly lower than in PR8 virus-infected BALB/c mice (Fig. 5C). In addition, the levels of CXCR3 and T-bet that were expressed by these Tregs were much more similar to those observed in RV6-infected HACII mice than was the case in PR8-infected BALB/c mice (Fig. 5D,E). Moreover, while the provision of Tregs led to a significant decrease in the accumulation of $CD4^+$Foxp3- and $CD8^+$ effector cells in the lungs of PR8-infected BALB/c mice, they did not cause similar reductions in RV6- or PR8-infected HACII mice (Fig. 5F). Thus, recognition of the self-HA in HACII mice both failed to support the efficient recruitment of HA-specific Tregs in virus-infected mice, and even prevented the accumulation and differentiation of these cells in response to a viral-Ag.

We considered the possibility that initial recognition of self-HA in a non-inflammatory context could impede the ability of Tregs to subsequently differentiate following TCR stimulation with viral-Ag during infection. To address this possibility, we infected HACII mice with RV6 virus, and then waited 4 d until the immune response to the virus was already underway prior to injecting $CD4^+Foxp3^+$ Tregs from TS1xHA28.$Foxp3^{eGFP}$.Ly5.1 mice. We then compared these mice with HACII mice into which $CD4^+Ly5.1^+$ Tregs had been transferred 1 d prior to RV6 infection (Fig. 6A). At d 8 p.i., a higher percentage of $Ly5.1^+$ Tregs expressed CXCR3 when the Tregs had been adoptively transferred 4 d p.i., rather than 1 d prior to infection, although they still did not reach the levels of CXCR3 expression that were found in PR8-infected BALB/c mice (Fig. 6B). This observation suggests that activation of the Tregs by self-HA in the context of viral infection-induced inflammation can result in enhanced Treg differentiation relative to that which occurs when the Tregs can interact with self-HA before the infection occurs. Nevertheless, despite this enhancement, the degree of CXCR3 and T-bet upregulation that occurred in response to the self-HA in virus-infected mice was still considerably reduced relative to that which could occur in response to viral-Ag in mice that do not express the HA as a self-Ag.

Treg differentiation is influenced by the type of APC that presents cognate Ag

It was also possible that the differing capacities of the HA to induce 6.5^+ Treg differentiation when expressed as a viral- versus a self-Ag could be due to its presentation by different APC subsets. To examine this, we first used flow cytometry to characterize the APC subsets present in the medLNs and lungs of RV6-infected HACII mice and PR8-infected BALB/c mice at d 6 p.i. (Supplementary Fig. 3). The numbers and distribution of a variety of APC subsets were quite similar in both sets of mice, and in each case, B cells were by far the most prevalent APC subset in the medLNs, and substantially outnumbered DCs in the lungs of infected mice (Fig. 7A,B). We also isolated DCs, B cells, neutrophils and inflammatory monocytes from the medLNs and lungs of both sets of mice, cultured them *in vitro* with CellTrace Violet-labeled LN cells from TS1xHA28 mice, and assessed

the division and CXCR3 expression of the $6.5^+CD4^+Foxp3^+$ Tregs after 4 d in culture. Very little division of the Tregs was observed when either neutrophils or inflammatory monocytes were used as APCs (data not shown). DCs isolated from either the lungs or the medLNs induced substantial Treg division, and in each case approximately half of the Tregs had upregulated CXCR3 (Fig. 7C,D). In PR8 infected BALB/c mice, B cells obtained from the lungs, but not from the medLNs induced Treg division. The ability of DCs, but not of B cells to stimulate Treg division in the medLNs at this stage of the infection in PR8-infected BALB/c mice is consistent with studies showing that immune responses to influenza virus are initiated in response to Ag that has been carried to the lung-draining LN by DCs (43, 44). By contrast, B cells obtained from both the medLNs and lungs of RV6-infected HACII mice were able to stimulate Treg division because in this case the HA is expressed and presented as a self-antigen by the B cells (Fig. 7C,D). Notably, however, in all cases, B cells induced very little up-regulation of CXCR3 despite inducing robust Treg proliferation, irrespective of whether the HA was being presented as a viral- or self-antigen. Moreover, CXCR3 was also less efficiently upregulated by the Tregs in intact medLNs of RV6-infected HACII mice than of PR8-infected BALB/c mice (Fig. 7E). Collectively, these studies suggest that the presence of large numbers of B cells expressing the self-HA can limit the degree of CXCR3 upregulation in a population of HA-specific Tregs even when DCs expressing the HA are also present, thus impairing their efficient trafficking to the lungs of RV6-infected HACII mice.

Discussion

We have examined how the immunostimulatory potency of a cognate Ag, the inflammatory environment, and the cell type by which the Ag is presented can affect $Foxp3^+$ Treg formation and differentiation *in vivo*. The formation and accumulation of HA-specific $6.5^+CD4^+Foxp3^+$ Tregs occurred more efficiently in HA28 mice than in HACII mice, and was associated with a weakly immunostimulatory mode of presentation of the HA self-Ag. Despite providing an environment that is favorable for 6.5^+ Treg formation and persistence, interactions with the self-HA in HA28 mice did not induce 6.5^+ Treg activity during influenza virus infection. In contrast, recognition of the HA as a viral-Ag drove Tregs to acquire a $CXCR3^+T\text{-}bet^+$ phenotype and suppress the anti-viral immune response. Notably, increasing the stimulatory capacity of the self-HA did not enable 6.5^+ Tregs to suppress the anti-viral immune response, and their ability to differentiate and enter the lungs of infected mice in response to viral-Ag was actually impaired by the expression of a highly immunostimulatory HA self-Ag by B cells.

Most of the work establishing that conventional $CD4^+Foxp3^-$ T cells can differentiate into $Foxp3^+$ Tregs in the periphery has been done using exogenously administered Ag (either through feeding or via injection) and/or studied in lymphopenic environments (6, 17–20, 45). However, the extent to which the continuous presence of endogenously synthesized, naturally processed self-Ags might also be able to promote pTreg formation in non-lymphopenic environments has not been extensively studied. Moreover, self-Ags can be either weakly or strongly immunogenic, and we found that differences in immunostimulatory potency could substantially affect the ability of the HA self-Ag to induce Treg cell formation. In the less immunostimulatory environment of HA28 mice, a

subset of HA-specific $CD4^+Foxp3^-$ T cells upregulated Foxp3 at d 3 post-transfer but had either remained undivided or had undergone 1 or 2 rounds of division, while the majority of $Foxp3^-$ cells had divided 3 to 5 times. In contrast, all of the HA-specific $CD4^+Foxp3^-$ T cells transferred into more strongly immunogenic HACII hosts had divided by d 3 post-transfer, with most having undergone more than 5 rounds of division, and no expression of Foxp3 was observed. These data are consistent with a previous study showing that injection of a low dose of cognate peptide induced more pTreg formation than a high dose, and that those cells that upregulated Foxp3 had undergone fewer rounds of division than those that did not (20). One explanation for these observations is that relatively weak activation of TCR signaling (such as occurs in HA28 mice) is more conducive to Treg formation than strong TCR signaling (in HACII mice), perhaps because the stronger signal more potently activates the PI3K/Akt/mTOR pathway downstream of the TCR, which has been shown to limit Foxp3 upregulation both *in vitro* and in the thymus (46, 47). However, if TCR signal strength is the sole determinant of pTreg formation, this would necessitate that some 6.5^+CD4^+ T cells in HA28 mice receive a relatively weak signal from the HA (becoming $Foxp3^+$ and undergoing limited division), while other cells receive a stronger signal from the HA self-peptide and divide more extensively without becoming $Foxp3^+$. Such differential signaling could arise if there is competition for the low levels of HA self-Ag that are expressed in HA28 mice; this might limit the exposure of a subset of the $6.5^+CD4^+Foxp3^-$ T cells to peptide:MHC complexes and promote Foxp3 upregulation selectively among these cells. Within the thymus, intraclonal competition for Ag has been suggested to occur based on observations that the formation of $CD4SPFoxp3^+$ thymocytes occurred most efficiently when there was a low frequency of thymocytes expressing TCRs that could promote selection into the Treg pathway (48, 59). Alternatively, there may be stochastic effects or epigenetic differences among the HA-specific $CD4^+Foxp3^-$ T cells that were introduced into the hosts and that allow only a subset of cells to upregulate Foxp3 upon initial Ag encounter, and the decreased proliferation of these cells relative to $Foxp3^-$ cells could be a consequence of the ability of Foxp3 to interact with downstream targets and induce a relatively non-proliferative (or “anergic”) state in those cells (49). A third possibility suggested by the relationship between Foxp3 expression and cell division that was observed at d 3 after transfer into HA28 mice is that the 6.5^+CD4^+ T cells were initially $Foxp3^+$, but then lost Foxp3 expression and underwent more extensive division. However, although only a minority of the 6.5^+CD4^+ T cells were $Foxp3^+$ at early times after transfer, by later time points they comprised nearly half of the congenically marked cells that could be recovered from HA28 mice. Since the total numbers of recovered cells were also declining at these later stages, it is likely that once acquired, Foxp3 expression was relatively stable in these pTregs, and that 6.5^+CD4^+ T cells that had undergone division without upregulating Foxp3 were gradually deleted, as has been observed in some other adoptive transfer settings (11). This stable expression of Foxp3 contrasts some findings in human and mouse systems in which Foxp3 was found to be transiently expressed by $CD4^+$ T cells at early stages following activation, and was not indicative of Treg development (50, 51). In this regard, it is noteworthy that although we found little or no evidence that $Foxp3^+$ Tregs were formed from 6.5^+CD4^+ T cells that had been transferred into HACII mice despite their extensive division, we also failed to obtain consistent engraftment unless the recipient HACII mice expressed a $Foxp3^{eGFP}$ allele. Although additional studies would be required to confirm this

conclusion, this observation provides indirect evidence that Foxp3 might be transiently expressed by these cells even though they do not ultimately convert into stable Foxp3$^+$ Tregs, and the concurrent expression of the GFP reporter transgene in conjunction with transient Foxp3 expression may mediate rejection in recipient mice that do not express GFP and therefore cannot induce tolerance to GFP as a self-Ag.

It was noteworthy that the 6.5$^+$CD4$^+$Foxp3$^+$ pTregs that were isolated from the pLNs of HA28 mice also acquired expression of Helios, the levels of which increased progressively following transfer, such that by d 14 and 21 the large majority of these cells were Helios$^+$. In unmanipulated mice, Helios is expressed in nearly all CD4SPFoxp3$^+$ cells in the thymus, but only about 70% of CD4$^+$Foxp3$^+$ cells in the periphery (39, 52). It was previously suggested that Helios is a marker for Tregs that had formed within the thymus, based mostly on observations that Helios was not upregulated in Ag-specific Tregs formed *in vitro* or *in vivo* by Ag feeding (39). This conclusion was challenged by subsequent studies showing that pTregs formed by i.v. injection of cognate Ag did express Helios, and it was unclear whether differences in the route of administration of an exogenous Ag might be causing these differences in Helios expression (52). We found that a significantly higher percentage of the 6.5$^+$CD4$^+$Foxp3$^+$ pTregs isolated from the mesLNs of HA28 mice were Helios$^-$ than was the case for those isolated from non-gut-draining pLNs. It is tempting to speculate that specialized CD103$^+$ DCs that reside in the gut and mesenteric LN and that can induce Treg differentiation via a TGF-β and retinoic acid dependent mechanism may be responsible for the development of Helios$^-$ pTregs (18, 19). Alternatively, elevated levels of TGF-β in the gut-draining mesLNs may promote their formation, since “induced” Foxp3$^+$ Tregs that are generated by activation of conventional CD4$^+$ T cells in the presence of TGF-β also lack Helios expression (39). Whatever the mechanism, these findings demonstrate that pTregs with identical specificity for a self-Ag can express different levels of Helios according to the anatomical location from which they are isolated.

Tregs have been shown to modulate immune responses to a variety of pathogens (7), but how TCR specificity for pathogen-derived and/or self-peptides can direct this activity is not well understood. We previously showed that 6.5$^+$CD4$^+$Foxp3$^+$ Tregs from TS1xHA28 mice could suppress the immune response to influenza virus infection based on the ability of the Tregs to recognize the S1 epitope of the HA as a viral-Ag (23), resembling studies in which CD4$^+$Foxp3$^+$ Tregs expressing a pathogen-specific transgenic TCR were found to modulate immune responses to *M. tuberculosis* (22). Notably, in both of these studies, the pathogens failed to induce the formation of Foxp3$^+$ pTregs from pathogen-specific conventional CD4$^+$ T cells, leading to the conclusion that Tregs that can modulate anti-pathogen immunity were generated prior to pathogen exposure (as opposed to acquiring Foxp3 during the course of the anti-pathogen response). However, many studies (including those in the TS1xHA28 system) have provided evidence that Tregs are formed predominantly in response to self-Ags, raising the question of whether Tregs might be able to modulate immune responses based on their ability to be activated by recognition of self-peptides that had induced their formation upon re-encounter in the inflammatory milieu of an infection (9–11, 53). We examined this possibility by infecting HA28 mice with the influenza virus RV6 with which 6.5$^+$CD4$^+$Foxp3$^+$ Tregs have very little reactivity; in contrast to PR8-infected BALB/c mice

(in which the HA is recognized as a viral-Ag and induces extension division of 6.5^+ Tregs in the medLNs of PR8-infected mice), 6.5^+ Tregs underwent much less division in RV6-infected BALB/c mice, and the presence of the self-HA in HA28 mice did not augment this division. Moreover, consistent with our previous report (23), activation of 6.5^+ Tregs was associated with significant upregulation of both CXCR3 and T-bet in the medLNs, followed by an accumulation of 6.5^+CXCR3$^+$T-bet$^+$ Tregs in the lungs of PR8-infected BALB/c mice, and suppression of the lung effector T cell response. By contrast, significantly lower levels of CXCR3 and T-bet were found in the 6.5^+CD4$^+$Foxp3$^+$ Tregs in the medLNs of RV6-infected HA28 or BALB/c mice, few of these cells trafficked to the lungs, and the effector T cell responses were not significantly affected. Thus, even though interactions with the self-HA as it is presented in HA28 mice can induce the formation of 6.5^+CD4$^+$Foxp3$^+$ Tregs both intrathymically and in the periphery, reactivity with this self-peptide was unable to induce activation of the Foxp3$^+$ Tregs sufficiently to allow them to modulate an acute influenza virus infection. In contrast, a similar number of Tregs with identical specificity could modulate anti-viral immunity when recognizing HA as a viral-Ag.

It was possible that the 6.5^+ Tregs failed to modulate anti-influenza virus immunity in response to the HA self-peptide in HA28 mice because the level of TCR stimulation induced by the self-peptide was too low to allow efficient activation in the infected mice, despite favoring Treg formation and persistence under steady state conditions. To evaluate the effects of increasing the degree of TCR stimulation by the HA self-peptide, we repeated these studies in HACII mice; this led to a similar degree of proliferation of the transferred Tregs as was found in PR8-infected BALB/c mice, but very few Tregs accumulated in the medLNs of uninfected HACII mice, and no upregulation of CXCR3 or T-bet occurred. When HACII mice were infected with the weakly crossreactive RV6 virus, 6.5^+ Tregs accumulated in increased numbers in the medLNs and a subset upregulated CXCR3 and T-bet and trafficked to the lungs. Based on previous studies using IFN-$\gamma R^{-/-}$ Tregs, it is likely that the high levels of IFN-γ induced by the RV6 virus infection prompted this CXCR3 upregulation and, coupled with the TCR response to the self-HA, promoted the formation of 6.5^+T-bet$^+$Foxp3$^+$ Tregs in HACII mice (27). However, this process occurred with significantly lower efficiency in RV6-infected HACII mice than in PR8-infected BALB/c mice, and the formation and trafficking of these predominantly self-reactive and virus-induced T-bet$^+$Foxp3$^+$ Tregs to the lungs did not significantly impair the anti-viral effector response.

Unexpectedly, the efficiency of 6.5^+T-bet$^+$Foxp3$^+$ Treg formation and its effects on anti-viral effector T cell formation were also substantially decreased in PR8-infected HACII mice relative to PR8-infected BALB/c mice; indeed, this process was no more efficient in PR8-infected HACII mice than in RV6-infected HACII mice, despite the ability of the transferred Tregs to receive a strong TCR signal from the viral-Ag. Two observations appear to account for the ability of the HA self-Ag to prevent 6.5^+ Tregs from modulating anti-viral immunity in HACII mice. First, we found that B cells that had been purified from RV6-infected HACII mice (presenting HA as a self-peptide) could induce extensive division of 6.5^+ Tregs while inducing only limited upregulation of CXCR3, resembling the phenotype that is observed when 6.5^+ Tregs are transferred into intact uninfected HACII mice. This appears to be a property of the presentation of a target Ag by B cells, because B cells

isolated from the lungs of PR8-infected BALB/c mice (i.e. B cells expressing the HA as a viral-Ag) similarly induced division of 6.5^+ Tregs with limited upregulation of CXCR3. By contrast, $CD11c^+$ DCs expressing either the viral- or self-HA efficiently induced both division of and CXCR3 upregulation by 6.5^+ Tregs. This difference in CXCR3 induction following activation by DCs versus B cells was presumably due to disparities in the costimulatory molecules and/or soluble factors such as cytokines that each cell type expresses (or induces) in the co-culture with $CD4^+Foxp3^-$ cells. Notably, B cells were previously found to be inefficient at promoting the induction of conventional Th1 $CD4^+$ cells, due in part to their inability to produce and/or promote production of IFN-γ, which is also necessary for induction of CXCR3 and T-bet by Tregs (27, 56–58). Moreover, B cells are by far the most abundant APC in both uninfected HACII mice and in the medLNs of influenza virus-infected mice, and these findings provide evidence that efficient presentation of an Ag by B cells can exert a dominant effect on the differentiation of Tregs even when DCs presenting the same Ag are also present. A corollary to this conclusion is that the ability of DCs to acquire antigen in the infected lung and migrate to the medLNs where they initiate immune responses in the absence of antigen-bearing B cells plays an important role in promoting the formation of Tregs that upregulate CXCR3 and can traffic back to the site of the infection (42–44).

Second, the inflammatory environment to which the Tregs are exposed at the time of initial Ag encounter appears to also contribute to their differentiation, because introduction of the 6.5^+ Tregs into HACII mice at the peak of an RV6 infection, rather than prior to infection, allowed a greater degree of CXCR3 upregulation to occur. When the 6.5^+ Tregs first encountered HA self-Ag in a HACII mouse that was already infected, CXCR3 upregulation was more efficient, indicating that TCR-induced division and exposure to inflammatory cytokines (such as IFN-γ) must occur concurrently to allow efficient Treg differentiation, although differentiation was still not as efficient as was the case for Tregs recognizing the viral-Ag in PR8-infected BALB/c mice. Together, these observations show that exposure of the 6.5^+ Tregs to the HA self-Ag that is expressed and presented by B cells in HACII mice before an infection was established could induce division of the Tregs without CXCR3 upregulation, and subsequent exposure to both the HA viral-Ag and the inflammatory environment of the infection could not induce these cells to become $CXCR3^+$ in PR8-infected HACII mice. Since acquisition of CXCR3 expression has been shown to direct $CD4^+$ T cell trafficking into infected lungs (54), it is likely that the lack of CXCR3 expression by the majority of 6.5^+ Tregs following activation in the medLN of infected HACII mice leads to the paucity of 6.5^+ Tregs that were present in the lungs of PR8-infected HACII mice. In this respect, it is noteworthy that the HA self-antigen is expressed by systemically distributed B cells in HACII mice, which causes Tregs to become activated both in the context of infection and at other sites in the body; it is possible that self-antigens whose expression is more restricted to the lungs could be less disruptive of CXCR3 upregulation, and might be better able to activate Treg activity in the lung environment. Ultimately, the studies presented here show that the activity of a Treg *in vivo* cannot necessarily be predicted based solely on its specificity for either a foreign or a self-Ag. Rather, the type of cell presenting Ag, the anatomical location, and the inflammatory environment at the time of initial antigenic encounter can all be factors that shape Treg

differentiation and activity, and will be important factors to understand when designing therapies based on the generation or adoptive transfer of Tregs.

Supplementary Material

Refer to Web version on PubMed Central for supplementary material.

Acknowledgments

We thank E. John Wherry for the provision of H-2K^{d}:Np147 tetramer, and the Wistar Flow Cytometry Core and Animal Facility for technical expertise.

This work was supported by NIH AI59166, NIH AI24541, NIH AI083022, NCI P30 CA10815, Sibley Memorial Hospital, and the Commonwealth of Pennsylvania. KAW was supported by NCI T32 CA09171.

Abbreviations used

Treg	regulatory T cell
HA	hemagglutinin
LN	lymph node
mesLN	mesenteric lymph node
pLN	peripheral (non-gut draining) lymph node
medLN	mediastinal lymph node
p.i	post-infection
pTreg	peripherally-derived regulatory T cell
tTreg	thymically-derived regulatory T cell
DC	dendritic cell

References

1. Sakaguchi S, Yamaguchi T, Nomura T, Ono M. Regulatory T cells and immune tolerance. Cell. 2008; 133:775–787. [PubMed: 18510923]
2. Vignali DA, Collison LW, Workman CJ. How regulatory T cells work. Nat Rev Immunol. 2008; 8:523–532. [PubMed: 18566595]
3. Fontenot JD, Gavin MA, Rudensky AY. Foxp3 programs the development and function of CD4+CD25+ regulatory T cells. Nat Immunol. 2003; 4:330–336. [PubMed: 12612578]
4. Bennett CL, Christie J, Ramsdell F, Brunkow ME, Ferguson PJ, Whitesell L, Kelly TE, Saulsbury FT, Chance PF, Ochs HD. The immune dysregulation, polyendocrinopathy, enteropathy, X-linked syndrome (IPEX) is caused by mutations of FOXP3. Nat Genet. 2001; 27:20–21. [PubMed: 11137993]
5. Wheeler KM, Samy ET, Tung KS. Cutting edge: normal regional lymph node enrichment of antigen-specific regulatory T cells with autoimmune disease-suppressive capacity. J Immunol. 2009; 183:7635–7638. [PubMed: 19923458]
6. Lathrop SK, Santacruz NA, Pham D, Luo J, Hsieh CS. Antigen-specific peripheral shaping of the natural regulatory T cell population. J Exp Med. 2008; 205:3105–3117. [PubMed: 19064700]
7. Maizels RM, Smith KA. Regulatory T cells in infection. Adv Immunol. 2011; 112:73–136. [PubMed: 22118407]

8. Campbell DJ, Koch MA. Phenotypical and functional specialization of FOXP3+ regulatory T cells. Nat Rev Immunol. 2011; 11:119–130. [PubMed: 21267013]
9. Jordan MS, Boesteanu A, Reed AJ, Petrone AL, Holenbeck AE, Lerman MA, Naji A, Caton AJ. Thymic selection of CD4+CD25+ regulatory T cells induced by an agonist self-peptide. Nat Immunol. 2001; 2:301–306. [PubMed: 11276200]
10. Apostolou I, Sarukhan A, Klein L, von Boehmer H. Origin of regulatory T cells with known specificity for antigen. Nat Immunol. 2002; 3:756–763. [PubMed: 12089509]
11. Walker LS, Chodos A, Eggena M, Dooms H, Abbas AK. Antigen-dependent proliferation of CD4+ CD25+ regulatory T cells in vivo. J Exp Med. 2003; 198:249–258. [PubMed: 12874258]
12. Picca CC, Oh S, Panarey L, Aitken M, Basehoar A, Caton AJ. Thymocyte deletion can bias Treg formation toward low-abundance self-peptide. Eur J Immunol. 2009; 39:3301–3306. [PubMed: 19768697]
13. Atibalentja DF, Byersdorfer CA, Unanue ER. Thymus-blood protein interactions are highly effective in negative selection and regulatory T cell induction. J Immunol. 2009; 183:7909–7918. [PubMed: 19933868]
14. Hsieh CS, Zheng Y, Liang Y, Fontenot JD, Rudensky AY. An intersection between the self-reactive regulatory and nonregulatory T cell receptor repertoires. Nat Immunol. 2006; 7:401–410. [PubMed: 16532000]
15. Josefowicz SZ, Niec RE, Kim HY, Treuting P, Chinen T, Zheng Y, Umetsu DT, Rudensky AY. Extrathymically generated regulatory T cells control mucosal TH2 inflammation. Nature. 2012; 482:395–399. [PubMed: 22318520]
16. Yadav M, Stephan S, Bluestone JA. Peripherally induced tregs - role in immune homeostasis and autoimmunity. Front Immunol. 2013; 4:232. [PubMed: 23966994]
17. Kretschmer K, Apostolou I, Hawiger D, Khazaie K, Nussenzweig MC, von Boehmer H. Inducing and expanding regulatory T cell populations by foreign antigen. Nat Immunol. 2005; 6:1219–1227. [PubMed: 16244650]
18. Coombes JL, Siddiqui KR, Arancibia-Carcamo CV, Hall J, Sun CM, Belkaid Y, Powrie F. A functionally specialized population of mucosal CD103+ DCs induces Foxp3+ regulatory T cells via a TGF-beta and retinoic acid-dependent mechanism. J Exp Med. 2007; 204:1757–1764. [PubMed: 17620361]
19. Sun CM, Hall JA, Blank RB, Bouladoux N, Oukka M, Mora JR, Belkaid Y. Small intestine lamina propria dendritic cells promote de novo generation of Foxp3 T reg cells via retinoic acid. J Exp Med. 2007; 204:1775–1785. [PubMed: 17620362]
20. Gottschalk RA, Corse E, Allison JP. TCR ligand density and affinity determine peripheral induction of Foxp3 in vivo. J Exp Med. 2010; 207:1701–1711. [PubMed: 20660617]
21. Suffia IJ, Reckling SK, Piccirillo CA, Goldszmid RS, Belkaid Y. Infected site-restricted Foxp3+ natural regulatory T cells are specific for microbial antigens. J Exp Med. 2006; 203:777–788. [PubMed: 16533885]
22. Shafiani S, Tucker-Heard G, Kariyone A, Takatsu K, Urdahl KB. Pathogen-specific regulatory T cells delay the arrival of effector T cells in the lung during early tuberculosis. J Exp Med. 2010; 207:1409–1420. [PubMed: 20547826]
23. Bedoya F, Cheng GS, Leibow A, Zakhary N, Weissler K, Garcia V, Aitken M, Kropf E, Garlick DS, Wherry EJ, Erikson J, Caton AJ. Viral antigen induces differentiation of Foxp3+ natural regulatory T cells in influenza virus-infected mice. J Immunol. 2013; 190:6115–6125. [PubMed: 23667113]
24. Shafiani S, Dinh C, Ertelt JM, Moguche AO, Siddiqui I, Smigiel KS, Sharma P, Campbell DJ, Way SS, Urdahl KB. Pathogen-specific Treg cells expand early during mycobacterium tuberculosis infection but are later eliminated in response to Interleukin-12. Immunity. 2013; 38:1261–1270. [PubMed: 23791647]
25. Zheng Y, Chaudhry A, Kas A, deRoos P, Kim JM, Chu TT, Corcoran L, Treuting P, Klein U, Rudensky AY. Regulatory T-cell suppressor program co-opts transcription factor IRF4 to control T(H)2 responses. Nature. 2009; 458:351–356. [PubMed: 19182775]

26. Chaudhry A, Rudra D, Treuting P, Samstein RM, Liang Y, Kas A, Rudensky AY. CD4+ regulatory T cells control TH17 responses in a Stat3-dependent manner. Science. 2009; 326:986–991. [PubMed: 19797626]
27. Koch MA, Tucker-Heard G, Perdue NR, Killebrew JR, Urdahl KB, Campbell DJ. The transcription factor T-bet controls regulatory T cell homeostasis and function during type 1 inflammation. Nat Immunol. 2009; 10:595–602. [PubMed: 19412181]
28. Cerasoli DM, Riley MP, Shih FF, Caton AJ. Genetic basis for T cell recognition of a major histocompatibility complex class II-restricted neo-self peptide. J Exp Med. 1995; 182:1327–1336. [PubMed: 7595203]
29. Shih FF, Cerasoli DM, Caton AJ. A major T cell determinant from the influenza virus hemagglutinin (HA) can be a cryptic self peptide in HA transgenic mice. Int Immunol. 1997; 9:249–261. [PubMed: 9040007]
30. Jordan MS, Riley MP, von Boehmer H, Caton AJ. Anergy and suppression regulate CD4(+) T cell responses to a self peptide. Eur J Immunol. 2000; 30:136–144. [PubMed: 10602035]
31. Haribhai D, Lin W, Relland LM, Truong N, Williams CB, Chatila TA. Regulatory T cells dynamically control the primary immune response to foreign antigen. J Immunol. 2007; 178:2961–2972. [PubMed: 17312141]
32. Hurwitz JL, Herber-Katz E, Hackett CJ, Gerhard W. Characterization of the murine TH response to influenza virus hemagglutinin: evidence for three major specificities. J Immunol. 1984; 133:3371–3377. [PubMed: 6208279]
33. Cozzo Picca C, Simons DM, Oh S, Aitken M, Perng OA, Mergenthaler C, Kropf E, Erikson J, Caton AJ. CD4(+)CD25(+)Foxp3(+) regulatory T cell formation requires more specific recognition of a self-peptide than thymocyte deletion. Proc Natl Acad Sci U S A. 2011; 108:14890–14895. [PubMed: 21873239]
34. Lerman MA, Larkin J 3rd, Cozzo C, Jordan MS, Caton AJ. CD4+ CD25+ regulatory T cell repertoire formation in response to varying expression of a neo-self-antigen. J Immunol. 2004; 173:236–244. [PubMed: 15210780]
35. Reed AJ, Noorchashm H, Rostami SY, Zarrabi Y, Perate AR, Jeganathan AN, Caton AJ, Naji A. Alloreactive CD4 T cell activation in vivo: an autonomous function of the indirect pathway of alloantigen presentation. J Immunol. 2003; 171:6502–6509. [PubMed: 14662850]
36. Kirberg J, Baron A, Jakob S, Rolink A, Karjalainen K, von Boehmer H. Thymic selection of CD8+ single positive cells with a class II major histocompatibility complex-restricted receptor. J Exp Med. 1994; 180:25–34. [PubMed: 8006585]
37. Webb S, Morris C, Sprent J. Extrathymic tolerance of mature T cells: clonal elimination as a consequence of immunity. Cell. 1990; 63:1249–1256. [PubMed: 2148123]
38. Apostolou I, von Boehmer H. In vivo instruction of suppressor commitment in naive T cells. J Exp Med. 2004; 199:1401–1408. [PubMed: 15148338]
39. Thornton AM, Korty PE, Tran DQ, Wohlfert EA, Murray PE, Belkaid Y, Shevach EM. Expression of Helios, an Ikaros transcription factor family member, differentiates thymic-derived from peripherally induced Foxp3+ T regulatory cells. J Immunol. 2010; 184:3433–3441. [PubMed: 20181882]
40. Haribhai D, Lin W, Edwards B, Ziegelbauer J, Salzman NH, Carlson MR, Li SH, Simpson PM, Chatila TA, Williams CB. A central role for induced regulatory T cells in tolerance induction in experimental colitis. J Immunol. 2009; 182:3461–3468. [PubMed: 19265124]
41. Hadis U, Wahl B, Schulz O, Hardtke-Wolenski M, Schippers A, Wagner N, Muller W, Sparwasser T, Forster R, Pabst O. Intestinal tolerance requires gut homing and expansion of FoxP3+ regulatory T cells in the lamina propria. Immunity. 2011; 34:237–246. [PubMed: 21333554]
42. Itano AA, Jenkins MK. Antigen presentation to naive CD4 T cells in the lymph node. Nat Immunol. 2003; 4:733–739. [PubMed: 12888794]
43. Legge KL, Braciale TJ. Accelerated migration of respiratory dendritic cells to the regional lymph nodes is limited to the early phase of pulmonary infection. Immunity. 2003; 18:265–277. [PubMed: 12594953]

44. Hamilton-Easton A, Eichelberger M. Virus-specific antigen presentation by different subsets of cells from lung and mediastinal lymph node tissues of influenza virus-infected mice. J Virol. 1995; 69:6359–6366. [PubMed: 7666537]
45. Knoechel B, Lohr J, Kahn E, Bluestone JA, Abbas AK. Sequential development of interleukin 2-dependent effector and regulatory T cells in response to endogenous systemic antigen. J Exp Med. 2005; 202:1375–1386. [PubMed: 16287710]
46. Haxhinasto S, Mathis D, Benoist C. The AKT-mTOR axis regulates de novo differentiation of CD4+Foxp3+ cells. J Exp Med. 2008; 205:565–574. [PubMed: 18283119]
47. Sauer S, Bruno L, Hertweck A, Finlay D, Leleu M, Spivakov M, Knight ZA, Cobb BS, Cantrell D, O'Connor E, Shokat KM, Fisher AG, Merkenschlager M. T cell receptor signaling controls Foxp3 expression via PI3K, Akt, and mTOR. Proc Natl Acad Sci U S A. 2008; 105:7797–7802. [PubMed: 18509048]
48. Bautista JL, Lio CW, Lathrop SK, Forbush K, Liang Y, Luo J, Rudensky AY, Hsieh CS. Intraclonal competition limits the fate determination of regulatory T cells in the thymus. Nat Immunol. 2009; 10:610–617. [PubMed: 19430476]
49. Hori S, Nomura T, Sakaguchi S. Control of regulatory T cell development by the transcription factor Foxp3. Science. 2003; 299:1057–1061. [PubMed: 12522256]
50. Wang J, Ioan-Facsinay A, van der Voort EI, Huizinga TW, Toes RE. Transient expression of FOXP3 in human activated nonregulatory CD4+ T cells. Eur J Immunol. 2007; 37:129–138. [PubMed: 17154262]
51. Miyao T, Floess S, Setoguchi R, Luche H, Fehling HJ, Waldmann H, Huehn J, Hori S. Plasticity of Foxp3(+) T cells reflects promiscuous Foxp3 expression in conventional T cells but not reprogramming of regulatory T cells. Immunity. 2012; 36:262–275. [PubMed: 22326580]
52. Gottschalk RA, Corse E, Allison JP. Expression of Helios in peripherally induced Foxp3+ regulatory T cells. J Immunol. 2012; 188:976–980. [PubMed: 22198953]
53. Hsieh CS, Liang Y, Tyznik AJ, Self SG, Liggitt D, Rudensky AY. Recognition of the peripheral self by naturally arising CD25+ CD4+ T cell receptors. Immunity. 2004; 21:267–277. [PubMed: 15308106]
54. Kohlmeier JE, Cookenham T, Miller SC, Roberts AD, Christensen JP, Thomsen AR, Woodland DL. CXCR3 directs antigen-specific effector CD4+ T cell migration to the lung during parainfluenza virus infection. J Immunol. 2009; 183:4378–4384. [PubMed: 19734208]
55. Caton AJ, Brownlee GG, Yewdell JW, Gerhard W. The antigenic structure of the influenza virus A/PR/8/34 hemagglutinin (H1 subtype). Cell. 1982; 31:417–427. [PubMed: 6186384]
56. Guery JC, Ria F, Galbiati F, Adorini L. Normal B cells fail to secrete interleukin-12. Eur J Immunol. 1997; 27:1632–1639. [PubMed: 9247571]
57. Stockinger B, Zal T, Zal A, Gray D. B cells solicit their own help from T cells. J Exp Med. 1996; 183:891–899. [PubMed: 8642293]
58. Maruo S, Oh-hora M, Ahn HJ, Ono S, Wysocka M, Kaneko Y, Yagita H, Okumura K, Kikutani H, Kishimoto T, Kobayashi M, Hamaoka T, Trinchieri G, Fujiwara H. B cells regulate CD40 ligand-induced IL-12 production in antigen-presenting cells (APC) during T cell/APC interactions. J Immunol. 1997; 158:120–126. [PubMed: 8977182]
59. Leung MW, Shen S, Lafaille JJ. TCR-dependent differentiation of thymic Foxp3+ cells is limited to small clonal sizes. J Exp Med. 2009; 206:2121–2130. [PubMed: 19737865]

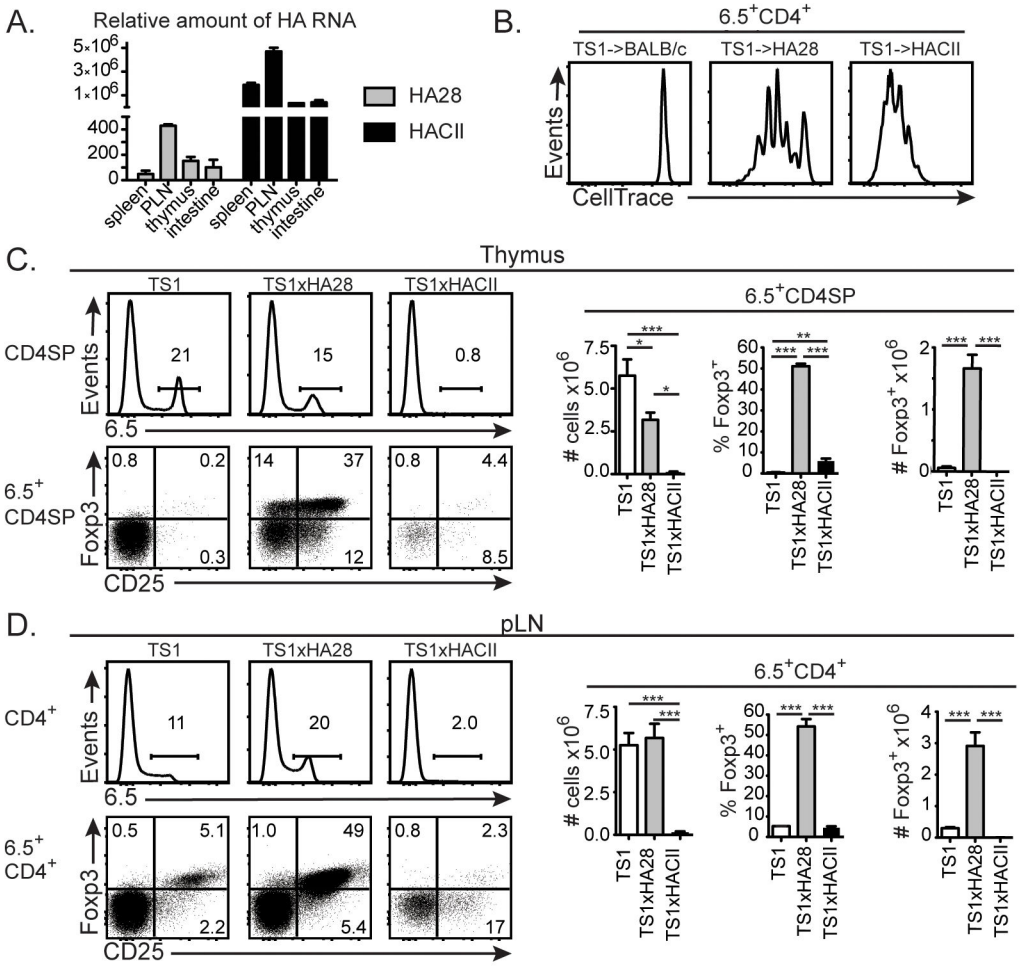

Figure 1. The immunostimulatory potency of the HA as a self-Ag determines the efficiency of 6.5$^+$ tTreg formation

(**A**) Graphs indicate mean levels of HA mRNA ±SEM in the indicated tissues of HA28 and HACII mice relative to RT-PCR signal generated using BALB/c RNA. Data from 3 independent experiments with tissues from 2 mice/group. (**B**) Histograms show levels of CellTrace Violet in 6.5$^+$CD4$^+$ cells from the pooled brachial, axillary and inguinal LNs of BALB/c, HA28 or HACII mice 3 d after receipt of CellTrace Violet-labeled CD4$^+$CD25$^-$eGFP$^-$ cells from TS1.Foxp3^{eGFP} mice (n=5–7 from 3 independent experiments). (**C**) Histograms show 6.5 expression by CD4SP thymocytes, and dot plots indicate CD25 versus Foxp3 expression by 6.5$^+$CD4SP thymocytes from TS1, TS1xHA28, and TS1xHACII mice. Graphs show mean numbers or percentages ±SEM of indicated cell types (n=4–6 from 3 independent experiment). (**D**) Same as (C), except for pLNs. For all panels percentages of cells in indicated gates are shown, and *=p<0.05; **=p<0.01; ***=p<0.005.

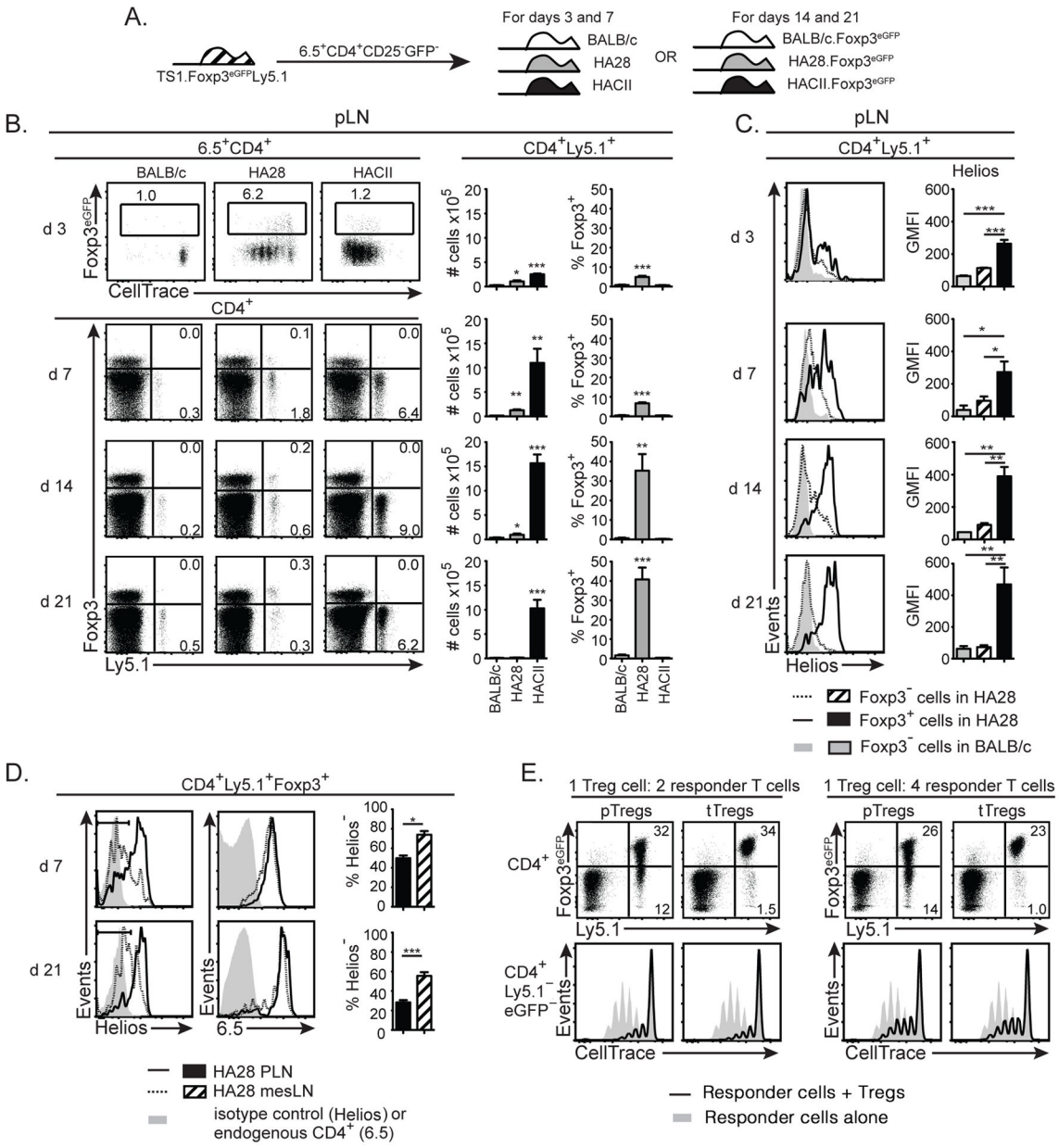

Figure 2. The immunostimulatory potency of the HA as a self-Ag determines the efficiency of conversion of 6.5$^+$CD4$^+$Foxp3$^-$ T cells into pTregs

(**A**) Schematic denotes transfer of 6.5$^+$CD4$^+$CD25$^-$eGFP$^-$ cells isolated from TS1.Foxp3^{eGFP}.Ly5.1 mice into BALB/c, HA28, and HACII hosts (or into BALB/c.Foxp3^{eGFP}, HA28.Foxp3^{eGFP}, and HACII.Foxp3^{eGFP} hosts for experiments terminating at d 14 or 21 post-transfer). (**B**) Upper panels show dot plots of eGFP versus CellTrace Violet levels on 6.5$^+$CD4$^+$ pLN cells isolated from BALB/c, HA28 and HACII mice 3 d post-transfer of CellTrace Violet-labeled 6.5$^+$CD4$^+$CD25$^-$eGFP$^-$ cells from TS1.Foxp3^{eGFP}.Ly5.1 mice. Lower panels show dot plots of Foxp3 versus Ly5.1 expression by CD4$^+$ pLN cells 7 d post-transfer of CellTrace Violet-labeled 6.5$^+$CD4$^+$CD25$^-$eGFP$^-$ cells from TS1.Foxp3^{eGFP}.Ly5.1 mice into BALB/c, HA28 and HACII mice, and 14 or 21 d

post-transfer into BALB/c.Foxp3^{eGFP}, HA28.Foxp3^{eGFP}, and HACII.Foxp3^{eGFP} mice. Graphs show mean numbers or percentages ±SEM of indicated cell types (n=4–8 for each recipient from at least 2 independent experiments at each time point). (**C**) Histograms show expression of Helios by indicated subsets of CD4^{+}Ly5.1^{+} pLN cells obtained from mice as described in (B). Graphs indicate geometric mean fluorescence intensity ±SEM of Helios staining. (**D**) Histograms show expression of Helios (left panels) or 6.5 (right panels) by CD4^{+}Ly5.1^{+}Foxp3^{+} cells isolated from the pLNs or mesLNs or HA28 mice 7 or 21 d post-transfer of 6.5^{+}CD4^{+}CD25^{-}eGFP^{-} cells from TS1.Foxp3^{eGFP}.Ly5.1 mice. Graphs show the mean percentages ±SEM of Helios^{-} cells from pLN versus mesLN (n=4 for d 7, n=7 for d 21). (**E**) Upper panels show dot plots of eGFP (Foxp3) versus Ly5.1 expression by CD4^{+} cells in cultures containing 6.5^{+}Ly5.1^{+}CD8^{-}eGFP^{+} cells that had been re-isolated from HA28 recipient mice 7 d after receiving 6.5^{+}CD4^{+}CD25^{-}eGFP^{-} cells from TS1.Foxp3^{eGFP}.Ly5.1 cells (labeled “pTregs”), or containing 6.5^{+}CD8^{-}Ly5.1^{+}eGFP^{+} cells from TS1xHA28.Foxp3^{eGFP}.Ly5.1 mice (labeled “tTregs”). In each case the Tregs were incubated with CellTrace Violet-labeled 6.5^{+}CD4^{+}eGFP^{-} responder T cells isolated from TS1.Foxp3^{eGFP} mice, along with S1 peptide and BALB/c splenocytes at a 1:2 or 1:4 ratio relative to responder T cells. Lower panels show histograms indicating the levels of CellTrace Violet staining by CD4^{+}Ly5.1^{-} responder T cells that had not been incubated with the Tregs (shaded histograms) or that had received either pTregs or tTregs (black lines). Data is representative of 2 independent experiments with pTregs pooled from 4–5 HA28 recipients for each experiment. For all panels percentages of cells in indicated gates are shown, and *=p<0.05; **=p<0.01; ***=p<0.005.

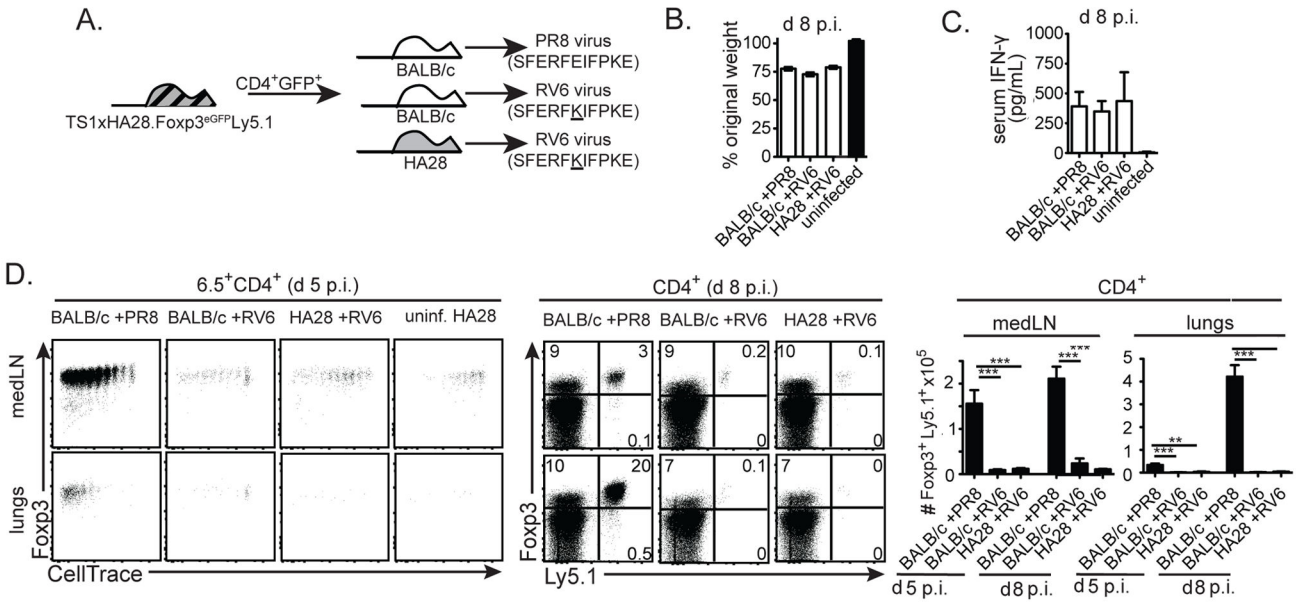

Figure 3. The HA self-Ag is unable to drive the expansion of 6.5$^+$ tTregs in HA28 mice infected with a non-cognate influenza virus

(**A**) Schematic denotes transfer of CD4$^+$eGFP$^+$ cells isolated from TS1xHA28.Foxp3^{eGFP}.Ly5.1 mice into BALB/c or HA28 mice, followed by infection 24 hours later with PR8 or RV6 viruses. (**B**) Graphs show mean percentages of original weight ±SEM of BALB/c or HA28 mice 8 d p.i. with indicated viruses (n=3–8). (**C**) Graphs show mean concentrations ±SEM of IFN-γ in the serum of BALB/c or HA28 mice 8 d p.i. with indicated viruses (n=6–9 for infected mice, n=3 for uninfected mice). (**D**) Left panels show dot plots of Foxp3 versus CellTrace Violet staining by 6.5$^+$CD4$^+$ cells obtained from medLNs or lungs 5 d after PR8 or RV6 infection of the indicated mouse strains that had received CellTrace Violet-labeled CD4$^+$GFP$^+$ cells from TS1xHA28.Foxp3^{eGFP}.Ly5.1 mice (uninf=uninfected). Middle panels show dot plots of Foxp3 versus Ly5.1 staining of CD4$^+$ medLN and lung cells obtained from similarly infected Treg-recipient mice at d 8 p.i.. Graphs indicate mean numbers ±SEM of CD4$^+$Foxp3$^+$Ly5.1$^+$ cells recovered from medLNs and lungs (n≥6 for each group).

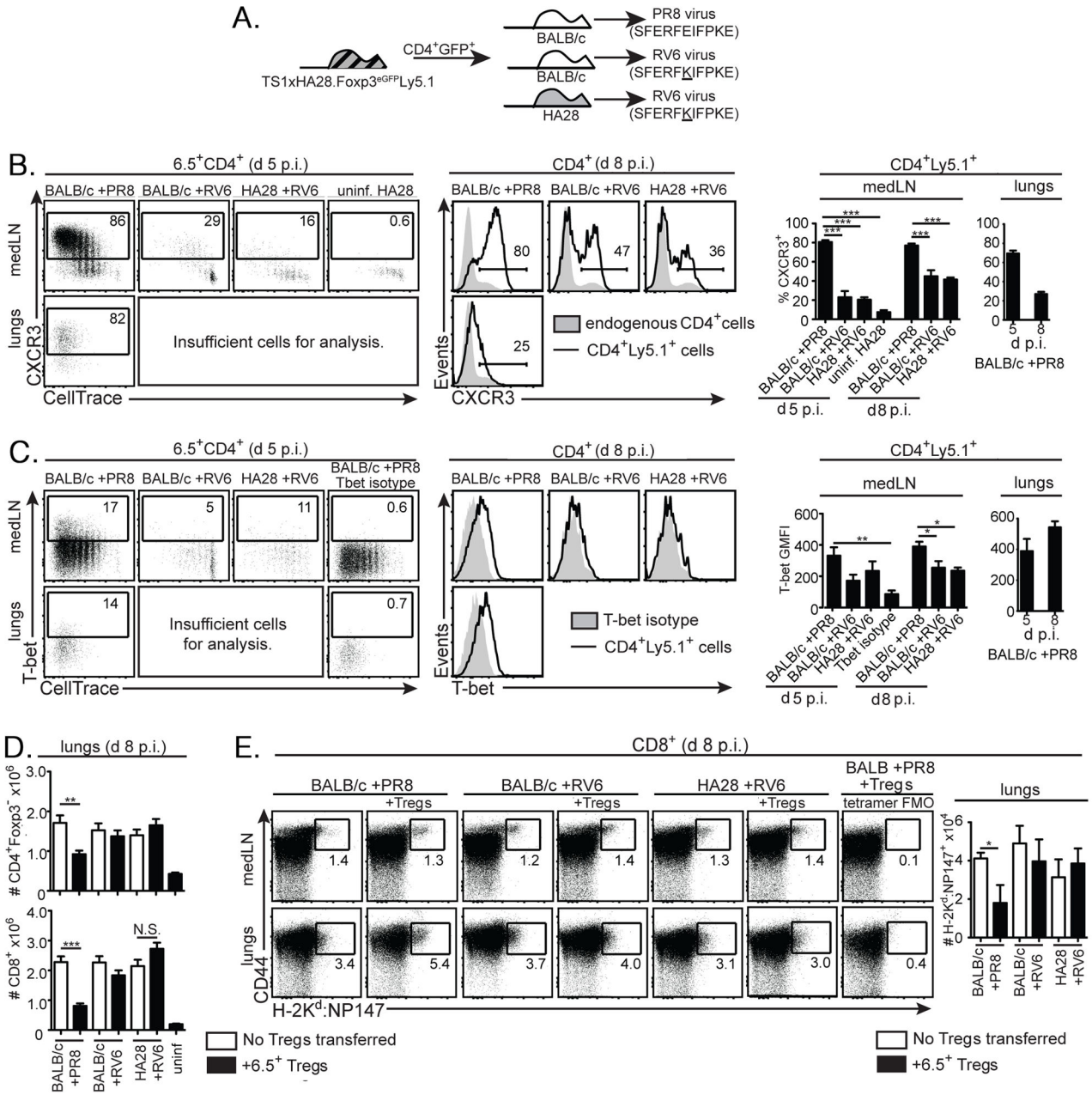

Figure 4.

In contrast to viral-Ag, the HA self-Ag is unable to drive the differentiation and activity of 6.5^+ tTregs in influenza virus-infected HA28 mice. (**A**) Schematic denotes transfer of $CD4^+eGFP^+$ cells isolated from TS1xHA28.Foxp3^{eGFP}.Ly5.1 mice into BALB/c or HA28 mice, followed by infection 24 hours later with PR8 or RV6 viruses. (**B**) Left panels show dot plots of CXCR3 versus CellTrace Violet staining by 6.5^+CD4^+ cells obtained from medLNs or lungs 5 d after PR8 or RV6 infection of the indicated mouse strains that had received CellTrace Violet-labeled $CD4^+GFP^+$ cells from TS1xHA28.Foxp3^{eGFP}.Ly5.1 mice. Samples containing insufficient cells for analysis are indicated. Middle panels show histograms of CXCR3 staining of $CD4^+Ly5.1^+$ cells (lines) overlaid with endogenous

$CD4^+Ly5.1^-$ cells (shaded histograms) isolated from medLNs and lungs of similarly infected Treg-recipient mice at d 8 p.i.. Right panels show graphs indicating the mean percentages ±SEM of $CD4^+Ly5.1^+$ cells that were $CXCR3^+$ in conditions shown in left and middle panels (n≥4 at d 5 p.i.; n≥6 at d 8 p.i. for each group). (**C**) As for (B), except that staining for T-bet is shown, including a sample in the left panel showing staining observed using an isotype control antibody instead of anti-T-bet. Graphs indicate geometric mean fluorescent intensity of T-bet staining. (**D**) Graphs show mean numbers ±SEM of $CD4^+Foxp3^-$ and $CD8^+$ effector cells obtained from the lungs 8 d after PR8 or RV6 infection of the indicated mouse strains that had (filled bars) or had not (open bars) received $6.5^+CD4^+GFP^+$ cells from TS1xHA28.$Foxp3^{eGFP}$.Ly5.1 mice (uninf=uninfected) (n≥6 for each group). (**E**) Dot plots show CD44 versus H-$2K^d$:NP147 tetramer staining in $CD8^+$ cells obtained 8 d after PR8 or RV6 infection of the indicated mouse strains that had ("+ Tregs") or had not received $CD4^+GFP^+$ cells from TS1xHA28.$Foxp3^{eGFP}$.Ly5.1 mice, including a sample showing the fluorescence minus one signal obtained in the tetramer channel for one of the samples. Graph shows the mean number of H-$2K^d$:$NP147^+CD44^+CD8^+$ cells obtained from the conditions shown in the histograms (n=3–4). For all panels percentages of cells in indicated gates are shown, and *=p<0.05; **=p<0.01; ***=p<0.005; NS= not significant.

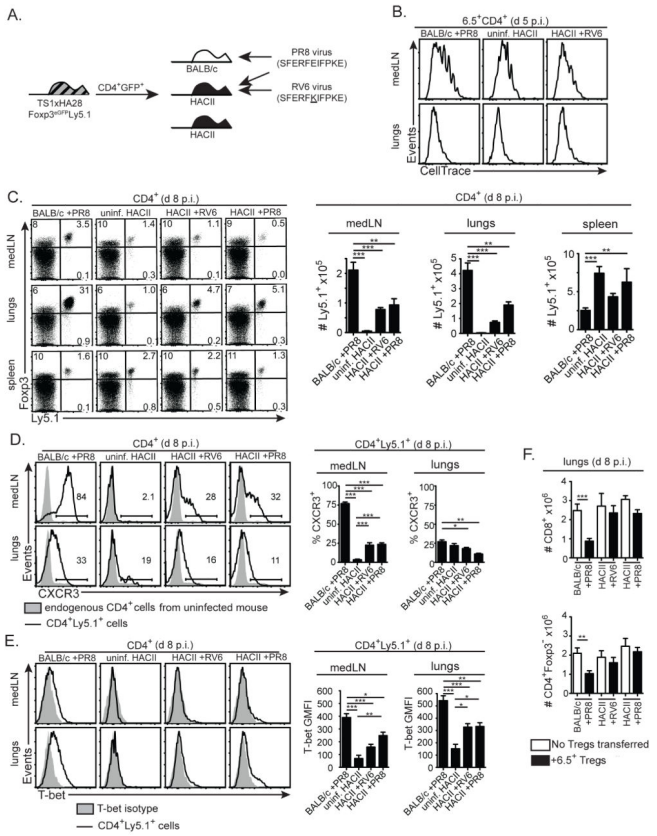

Figure 5.

A strongly immunostimulatory HA self-Ag inhibits the differentiation and activity of Tregs responding to the viral-Ag during influenza virus infection. (**A**) Schematic denotes transfer of $CD4^+eGFP^+$ cells isolated from TS1xHA28.Foxp3^{eGFP}.Ly5.1 mice into BALB/c or HACII mice, followed in some cases by infection 24 hours later with PR8 or RV6 viruses. (**B**) Histograms show CellTrace Violet staining by 6.5^+CD4^+ cells isolated from the medLNs or lungs of BALB/c mice that had been infected with PR8 virus, or from HACII mice that were uninfected or had been infected with RV6 virus. The day after infection, mice had received CellTrace Violet-labeled $CD4^+eGFP^+$ cells isolated from TS1xHA28.Foxp3^{eGFP}.Ly5.1 mice, and cells were isolated and analyzed after 4 additional days. (**C**) Dot plots show Foxp3 versus Ly5.1 staining by $CD4^+$ cells obtained from medLNs, lungs or spleens 8 d after PR8 or RV6 infection of the indicated mouse strains that had received CellTrace Violet-labeled $CD4^+GFP^+$ cells from TS1xHA28.Foxp3^{eGFP}.Ly5.1 mice. Graphs show the mean numbers ±SEM of $CD4^+Ly5.1^+$ cells that were isolated from indicated tissues in the different conditions. (**D**) Histograms show CXCR3 staining of $CD4^+Ly5.1^+$ cells (lines) overlaid with endogenous $CD4^+Ly5.1^-$ cells (shaded histograms) isolated from medLNs, lungs or spleens 8 d after PR8 or RV6 infection of the indicated mouse strains that had received $CD4^+GFP^+$ cells from TS1xHA28.Foxp3^{eGFP}.Ly5.1 mice. Graphs indicate the mean percentages ±SEM of $CD4^+Ly5.1^+$ cells that were $CXCR3^+$ in each condition (n≥5 for each group). (**E**) As for (D), except that staining for T-bet by $CD4^+Ly5.1^+$ cells is shown (lines) overlaying staining observed with a T-bet isotype control

instead of anti-T-bet (shaded histograms). Graphs indicate geometric mean fluorescent intensity ±SEM of T-bet staining (n≥5 for each group). (**F**) Graphs show mean numbers ±SEM of $CD4^+Foxp3^-$ and $CD8^+$ effector cells obtained from the lungs 8 d after PR8 or RV6 infection of the indicated mouse strains that had (filled bars) or had not (open bars) received $6.5^+CD4^+GFP^+$ cells from TS1xHA28.$Foxp3^{eGFP}$.Ly5.1 mice (n≥5 for each group). For all panels percentages of cells in indicated gates are shown, and *=p<0.05; **=p<0.01; ***=p<0.005.

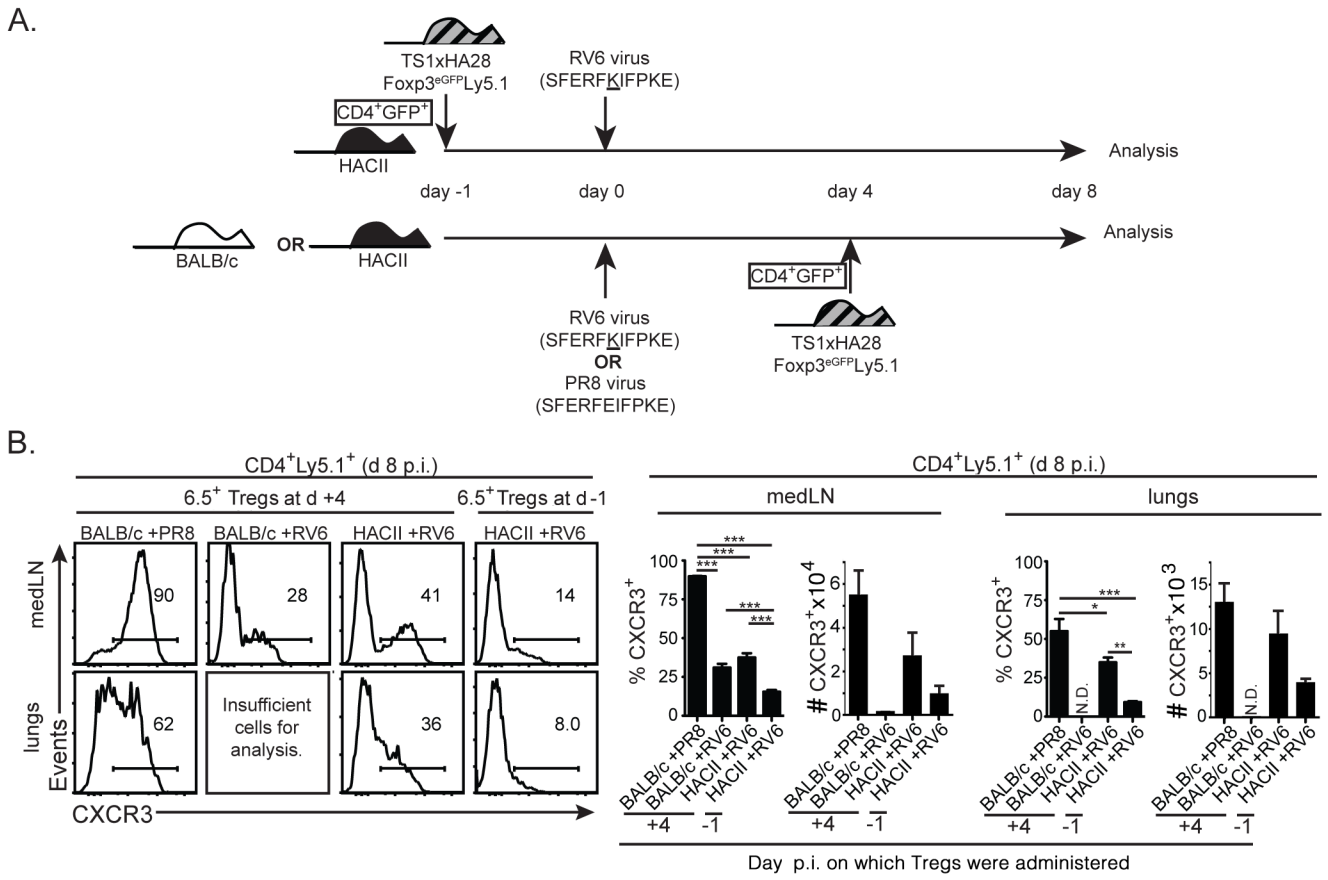

Figure 6.

Infection-associated inflammation partially overcomes the ability of self-HA to inhibit CXCR3 upregulation by Tregs responding to viral-Ag. (**A**) Schematic denotes transfer of $CD4^+eGFP^+$ cells isolated from TS1xHA28.Foxp3^{eGFP}.Ly5.1 mice into HACII mice followed 24 hours later by RV6 infection and analysis at d 8 p.i.. Alternatively, these cells were transferred into BALB/c or HACII mice 4 d after infection with PR8 virus, and analyzed after 4 additional days (i.e. at d 8 p.i.). (**B**) Histograms show CXCR3 expression by $Ly5.1^+CD4^+$ cells isolated from the medLN and lungs 8 d after PR8 or RV6 infection of the indicated mouse strains that had received $CD4^+GFP^+$ cells from TS1xHA28.Foxp3^{eGFP}.Ly5.1 mice either 1 d before ("d −1"), or 4 d after ("d +4") infection. Graphs indicate the mean percentages and numbers ±SEM of $CD4^+Ly5.1^+$ cells that were $CXCR3^+$ in these conditions (n≥5 for each group). Percentages of cells in indicated gates are shown, and *=p<0.05; **=p<0.01; ***=p<0.005.

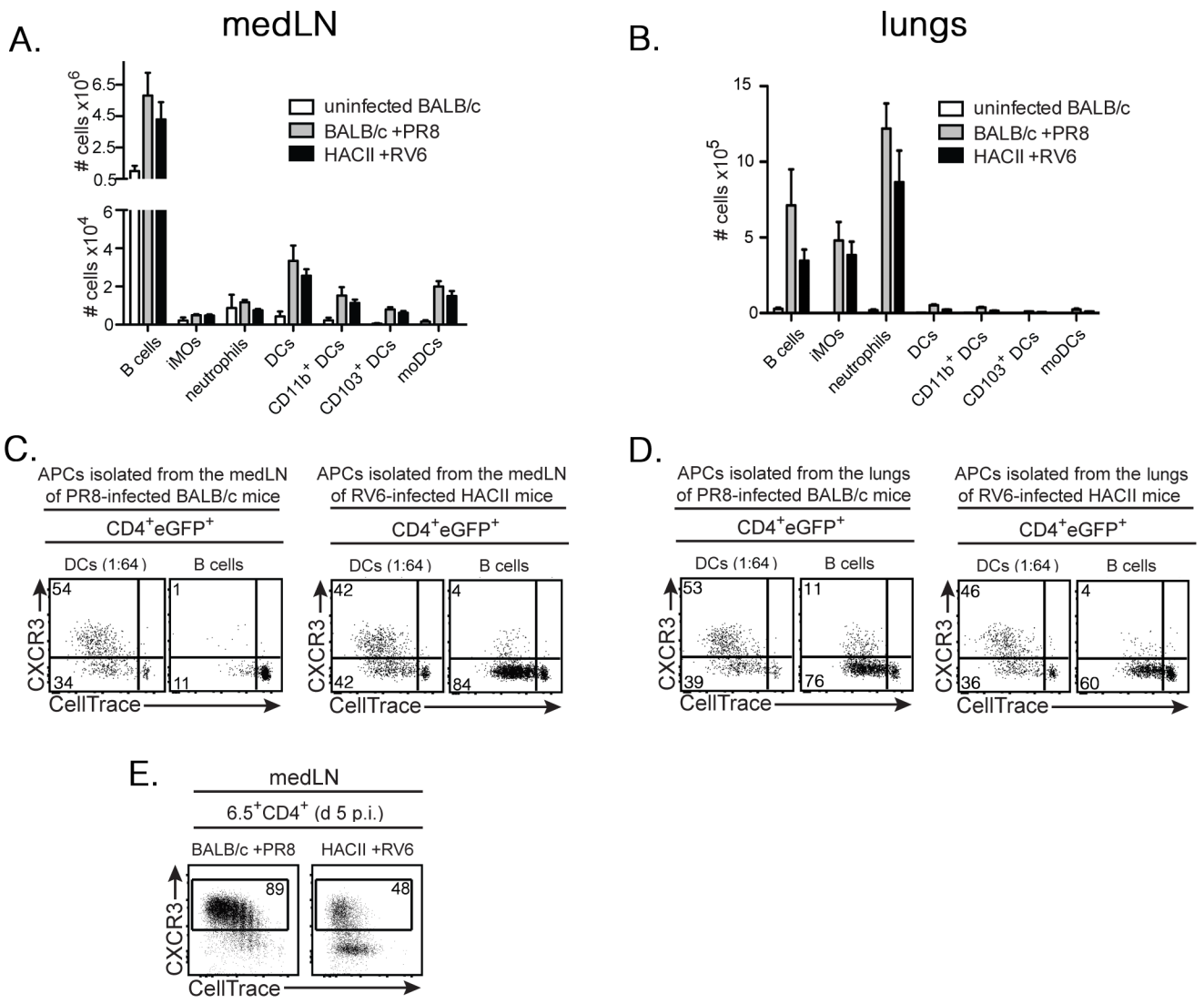

Figure 7.

B cells and DCs have differing capacities to induce upregulation of CXCR3 by Tregs responding to HA self-Ag. (**A**) Graph shows mean numbers ±SEM of B cells ($CD19^+CD11c^-CD11b^-$), inflammatory monocytes ("iMOs": $CD19^-CD11c^-CD11b^+Ly6G^-Ly6C^{hi}$), neutrophils ($CD19^-CD11c^-CD11b^+Ly6G^{hi}Ly6C^{lo}$), total DCs ($CD19^-CD11c^+Ly6C^-Ly6G^-$), $CD11b^+$ DCs ($CD19^-CD11c^+Ly6C^-Ly6G^-CD11b^+CD103^-$), $CD103^+$ DCs ($CD19^-CD11c^+Ly6C^-Ly6G^-CD103^+$) and monocyte-derived DCs ("moDCs"; $CD19^-CD11c^+Ly6C^+Ly6G^-$) (see Supplementary Fig. 3) isolated from the medLNs of uninfected BALB/c mice, or from BALB/c or HACII mice 6 d p.i. with PR8 or RV6, respectively (n=3 for each condition). (**B**) As for (A), except lungs were analyzed. (**C**) Dot plots show staining for CXCR3 versus CellTrace Violet by $CD4^+eGFP^+$ cells following incubation of CellTrace Violet-labeled LN cells from TS1xHA28.$Foxp3^{eGFP}$ mice for 4 d with DCs (diluted 1:64 with $CD4^-CD8^-$ BALB/c splenocytes) or B cells isolated from the medLNs of PR8-infected BALB/c mice (left panels) or RV6-infected HACII mice (right

panels) at d 6 p.i. Numbers show percentages of cells in indicated gates. Data are from 1 representative of 3 independent experiments, in which LNs from 4 mice were pooled prior to isolation of DCs and B cells. (**D**) As for (C), except lungs were analyzed. (**E**) Dot plots show CXCR3 versus CellTrace Violet staining by $6.5^{+}CD4^{+}$ cells in the medLNs of BALB/c and HACII mice that had each received CellTrace Violet-labeled $CD4^{+}eGFP^{+}$ cells isolated from TS1xHA28.$Foxp3^{eGFP}$.Ly5.1 mice, infected with PR8 or RV6 virus, and then analyzed 5 d later. Percentages of cells that are $CXCR3^{+}$ are shown.